IN THE UNITED STATES PATENT AND TRADEMARK OFFICE
PATENT EXAMINING OPERATION

Applicant(s):	Lukas et al.		
Serial No.:	10/624,356	**Group Art Unit:**	1762
Filed:	21 July 2003	**Examiner:**	M. Padgett
Atty. Docket No.:	06336P USA	**Confirmation No.:**	7682
For:	NON-THERMAL PROCESS FOR FORMING POROUS LOW DIELECTRIC COONSTANT FILMS		

DECLARATION UNDER 37 C.F.R. § 1.132

Commissioner for Patents
P.O. Box 1450
Alexandria, VA 22313-1450

Sir:

I, Mark O'Neill, Ph.D., a citizen of Canada hereby declare and state:

1. I have a Bachelor's of Science in Chemistry and a Ph.D. in Physical Chemistry from Carlton University in Ottawa, Ontario.

2. I am currently employed by Air Products and Chemicals, Inc. (APCI), the assignee of the present application. I have been employed by APCI for approximately 9 years. My present position is Lead Research Chemist. In this capacity I lead a team of researchers and engineers in the development of new materials and processes for microelectronic device manufacturing.

3. I am a co-inventor on the present application, U.S. patent application Serial No. 10/624,356 ("the 356 application"), along with Aaron Lukas, Mark Bitner, Jean Vincent, Raymond Vrtis, and Eugene Karwacki.

4. I have reviewed the 356 application, which I understand to have been filed in the United States Patent & Trademark Office on July 21, 2003, as well as copies of the Final Office Action dated May 19, 2006 ("the Final Action"). I have also reviewed the references cited in this correspondence, namely, U.S. Patent No.5,935,646 to Raman et al. ("Raman") in view of U.S.

patent application Publication No. 2003/0054115 to Albano et al. ("Albano"); U.S. patent application Publication No. 2003/0003288 to Nakata et al. ("Nakata"); and Raman in view of Albano and further in view of Nakata. I have also reviewed the Reply to which this declaration is attached.

5. I understand that independent Claim 1 has been amended to define a process for preparing a porous film, the process comprising the steps of: forming a composite film onto at least a portion of a substrate wherein the composite film comprises at least one silicon-based structure-forming material and at least one pore-forming material, and wherein the composite film is substantially free of Si-OH bonds; and exposing the composite film to at least one ultraviolet light source within a non-oxidizing atmosphere for a time sufficient to remove at least a portion of the at least one pore-forming material contained therein and provide the porous film.

6. I understand that independent Claim 28 has been amended to define a process for preparing a porous film, the process comprising: forming a composite film onto at least a portion of a substrate wherein the composite film comprises at least one silicon-based structure-forming material and at least one pore-forming material, and wherein the composite film is substantially free of Si-OH bonds; exposing the composite film to at least one energy source comprising ultraviolet light within a non-oxidizing atmosphere for a time sufficient to remove at least a portion of the at least one pore-forming material contained therein to provide the porous film; and treating the porous film with one or more second energy sources.

7. I understand that independent Claim 37 has been amended to define a process for preparing a porous film, the process comprising: forming a composite film onto at least a portion of a substrate wherein the composite film comprises at least one silicon-based structure-forming material and at least one pore-forming material, and wherein the composite film is substantially free of Si-OH bonds; and exposing the composite film to an ultraviolet light source within a non-oxidizing atmosphere for a time sufficient to remove at least a portion of the at least one pore-

forming material contained therein to provide the porous film wherein the density of the porous film is at least 10% less than the density of the composite film.

8. I understand that independent Claim 38 has been amended to define a process for preparing a porous film, the process comprising: forming a composite film having a first density onto at least a portion of a substrate wherein the composite film comprises at least one silica-based structure-forming material and at least one pore-forming material, and wherein the composite film is substantially free of Si-OH bonds; and exposing the composite film to an ultraviolet light source within a non-oxidizing atmosphere for a time sufficient to substantially remove the at least one pore-forming material contained therein to provide the porous film having a second density wherein the second density is at least 10 percent less than the first density.

9. I understand that independent Claim 42, the final independent claim in the 356 application, has been amended to define a chemical vapor deposition method for producing a porous film represented by the formula $Si_vO_wC_xH_yF_z$, where v+w+x+y+z = 100 atomic%, v is from 10 to 35 atomic%, w is from 10 to 65 atomic%, x is from 5 to 30 atomic%, y is from 10 to 50 atomic%, and z is from 0 to 15 atomic%, the method comprising: providing a substrate within a vacuum chamber; introducing into the vacuum chamber gaseous reagents including at least one structure-forming precursor gas selected from the group consisting of an organosilane and an organosiloxane, and a pore-former precursor distinct from the at least one structure-forming precursor; applying energy to the gaseous reagents in the vacuum chamber to induce reaction of the precursors to deposit a composite film on the substrate, wherein the composite film comprises at least one structure-forming material and at least one pore-forming material, and wherein the composite film is substantially free of Si-OH bonds; and exposing the composite film to an ultraviolet light source within a non-oxidizing atmosphere for a time sufficient to substantially remove the at least one pore-forming material contained therein to provide the porous film comprising a plurality of pores and a dielectric constant of 2.7 or less.

10. I understand from the Final Action that the Patent Office has asserted that the claims of the 356 application are unpatentable because the differences between the claimed invention and the cited references (*i.e.*, Raman, Albano, and Nakata) are such that the claimed invention would have been obvious at the time that the methods were invented to a person having ordinary skill in the field to which the claimed invention pertains.

11. I do not agree with the Patent Office that the differences between the claimed invention and the cited references are such that the claimed invention would have been obvious at the time that the invention was made to a person having ordinary skill in the field to which the claimed invention pertains. In this regard, the cited references – either alone or in combination do not teach or suggest a forming composite film comprising at least one silicon-based structure-forming material and at least one pore-forming material, and wherein the composite film is substantially free of Si-OH bonds.

12. The porous films disclosed in Raman, Nakata, and Albano are ***not*** substantially free of Si-OH bonds. Significantly, the porous films disclosed in each of the cited references are prepared by applying a wet coat of a structure-forming material prepared by co-polymerizing tetraethoxysilane (TEOS) and methyltriethoxysilane (MTES) dissolved in ethanol in a two-step acid catalyzed procedure (*see*, Raman at col. 8, lines 33 to 42; Albano at [0064] to [0070]; and Nakata at page 4, paragraph [0081]). Such condensation reactions ***necessarily results*** in the formation of a siloxane polymer having Si-OH bonds (See, Exhibit A at page 130, section 2.3.5 and 2.3.6).

13. Exhibit A attached to my declaration included excerpts from a well-known text book entitled "Sol-Gel Science, The Physics and Chemistry of Sol-Gel Processing" by C. Jeffrey Brinker and George W. Scherer ("the Sol-Gel reference"). Interestingly, one of the co-authors of the Sol-Gel reference is C. Jeffrey Brinker who is also a co-inventor on Raman. The Sol-Gel reference, and in particular, chapters 2.3.5.1 to 2.5, shows that the formation of Si-OH groups is an intermediate step to the formation of polymeric siloxanes.

14. The formation of polymeric siloxanes is a kinetically limited process whereby the completion of cross-linking inherently cannot achieve 100% conversion of Si-OH to Si-O-Si species. According to the Sol-Gel reference at page 577, for example, only when a silica polymer is thermally annealed to temperatures near 1100°C will the majority of the residual Si-OH species be annealed from the matrix. The thermal budget for the manufacture of semiconductor structures that will employ porous low dielectric constant materials is limited to temperatures of less than 400°C. Therefore, silicate polymers formed by a sol-gel method will inherently contain measurable quantities of Si-OH that may render the film hygroscopic, as suggested by Nakata (page 1, para 17).

15. In contrast, the present invention provides a process for preparing a porous film wherein a composite film is formed comprising at least one silicon-based structure-forming material and at least one pore-forming material wherein the composite film is substantially free of Si-OH bonds. See, for example, the IR spectra of Figure 2 of the 356 application wherein there is no significant –OH peak and compare with the IR spectra of Figure 3, which shows a significant peak of the final film that was formed in the presence of oxygen.

16. Thus, there are significant differences between the inventions defined by the above-identified independent claims and the teachings of the cited references whether each reference is considered alone or in combination with the others.

17. I hereby declare that all statements made herein of my own knowledge are true, and that all statements made on information and belief are believed to be true; and further that these statements were made with the knowledge that willful false statements and the like so made are punishable by fine and/or imprisonment under Section 1001 of Title 18 of the United States Code, and that such willful false statements may jeopardize the validity of the application or any patent issuing therefrom.

Date: Oct. 9, 2006

Mark L. O'Neill, Ph.D.

EXHIBIT A

SOL-GEL SCIENCE

The Physics and Chemistry of Sol-Gel Processing

SOL-GEL SCIENCE

The Physics and Chemistry of Sol-Gel Processing

C. Jeffrey Brinker

Sandia National Laboratories
Albuquerque, New Mexico

George W. Scherer

E. I. du Pont de Nemours & Company
Wilmington, Delaware

ACADEMIC PRESS, INC.

Harcourt Brace Jovanovich, Publishers

Boston San Diego New York
London Sydney Tokyo Toronto

This book is printed on acid-free paper. ♾

ACADEMIC PRESS, INC.
1250 Sixth Avenue, San Diego, CA 92101

United Kingdom Edition published by
ACADEMIC PRESS LIMITED.
24–28 Oval Road, London NW1 7DX

Library of Congress Cataloging-in-Publication Data

Brinker, C. Jeffrey.
Sol-gel science : the physics and chemistry of sol-gel processing
/ C. Jeffrey Brinker, George W. Scherer.
p. cm.
Includes bibliographical references.
ISBN 0-12-134970-5 (alk. paper)
1. Ceramic materials. 2. Colloids. I. Scherer, George W.
II. Title.
TP810.5.B75 1990
666—dc20 89-15631
CIP

Printed in the United States of America
90 91 92 93 9 8 7 6 5 4 3 2 1

Fig. 16.

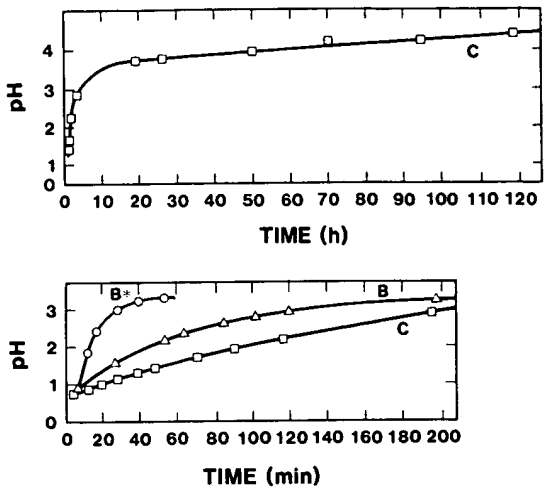

pH versus time during B: acid-catalyzed hydrolysis of TMOS at room temperature in methanol–formamide solutions, TEOS : EtOH : H_2O : HNO_3 : CH_3NO = 1:3:10:0.3:3; B* = 60°C; C: acid-catalyzed hydrolysis of formamide, EtOH : H_2O : HNO_3 : CH_3NO = 3:10:0.3:3. Upper curve: 60°C; lower curve: room temperature [72].

[e.g., 49,50,60], although by analogy to carbon chemistry *siliconium ions*, $Si(OR)_3^+$, have also been suggested as possible intermediates [61].

2.3.5.1. Acid-catalyzed Hydrolysis

Under acidic conditions, it is likely that an alkoxide group is protonated in a rapid first step. Electron density is withdrawn from silicon, making it more electrophilic and thus more susceptible to attack by water. Pohl and Osterholz [50] favor a transition state with significant S_N2-type character. The water molecule attacks from the rear and acquires a partial positive charge. The positive charge of the protonated alkoxide is correspondingly reduced, making alcohol a better *leaving group*. The transition state decays by displacement of alcohol accompanied by *inversion* of the silicon tetrahedon:

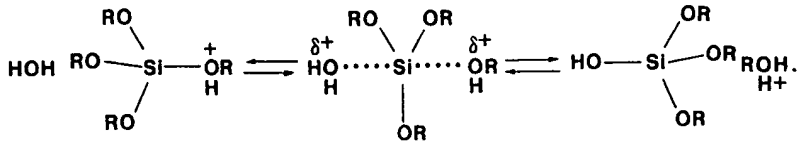

(25)

Consistent with this mechanism, the hydrolysis rate is increased by substituents that reduce steric crowding around silicon (Fig. 11 and Table 6). Electron-providing substituents (e.g., alkyl groups) that help stabilize the developing positive charges should also increase the hydrolysis rate (Fig. 13) but to a lesser extent, because the silicon acquires little charge in the transition state.

Keefer [48] has discussed possible consequences of inversion of the silicon tetrahedron with regard to retarding the hydrolysis of silicate species that are contained in polymers. Using optically active monomers $R'_xSi^*(OR)_{4-x}$, Sommer and coworkers [73–75] have proven that inversion occurs during hydrolysis of several monomers including $R_3Si^*OCH_3$. As a general rule, inversion occurs in displacement reactions with good leaving groups such as Cl^- or $OCOR^-$ whose *conjugate acids* (corresponding protonated anions) have $pK_a < 6$, regardless of the nature of the solvent provided that the attacking reagent furnishes an entering group more basic than the leaving group [75]. For poorer leaving groups such as H or OR whose conjugate acids have $pK_a > 6$, retention or inversion may occur depending on the nature of the catalyst cation and the solvent polarity. For example, hydrogen bonding of the solvent may facilitate inversion by activating poor leaving groups [47]:

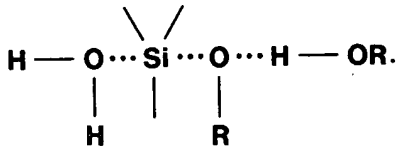

(26)

Klemperer and coworkers [38] have shown that, under neutral conditions, constrained oligomers (cubic octamers) hydrolyze without inversion. (See pathway A, Fig. 17.) This suggests that retention or inversion is further influenced by specific bonding configurations.

Several investigators have proposed hydrolysis mechanisms involving flank-side attack without inversion of the silicon tetrahedron [48,76]. A possible acid-catalyzed mechanism is the following:

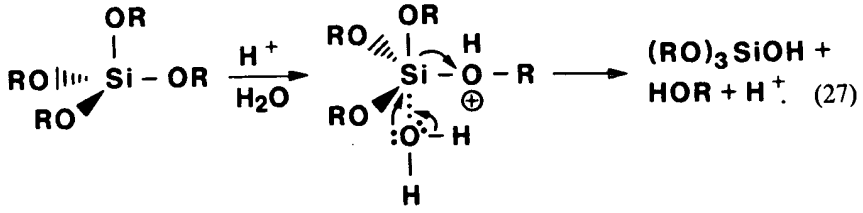

(27)

This mechanism is subject to both steric and inductive effects. Compared to the S_N2 mechanism described previously, electron-providing substituents

Fig. 17.

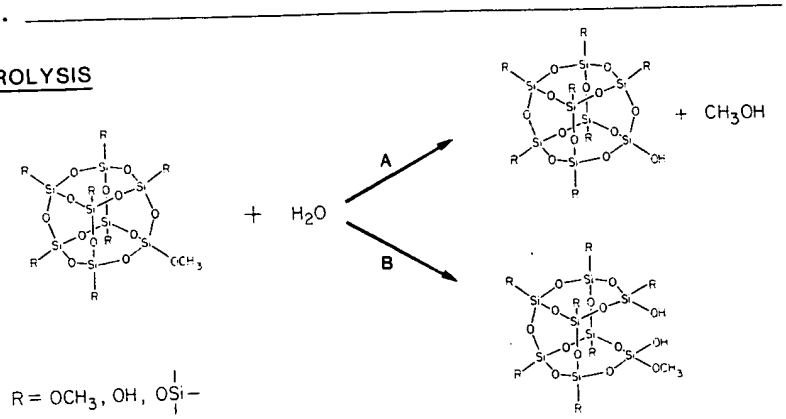

Possible pathways for hydrolysis of methoxy terminated Q^3 species contained in cubic octamers: A) with retention of configuration, B) with siloxane bond hydrolysis [38].

should have a greater effect, because the silicon acquires more charge in the transition state.

Timms [77] has proposed an acid-catalyzed hydrolysis mechanism involving a siliconium ion ($\equiv Si^+$). An alkoxide group is rapidly protonated followed by a slower step in which a siliconium ion is formed by the removal of alcohol:

$$\equiv Si-OR + H^+ \rightleftharpoons \equiv Si-\underset{H^+}{OR} \xrightarrow{SLOW} \equiv Si^+ + ROH, \qquad (28)$$

$$\equiv Si^+ + ROH \overset{H_2O}{\rightleftharpoons} \equiv Si-OH + ROH + H^+. \qquad (29)$$

Water reacts with the siliconium ion to form a silanol and the proton is regenerated (Eq. 29). Consistent with the observed behavior, this reaction should have third-order overall kinetics and should be accelerated by electron-providing substituents attached to silicon (Figs. 12 and 13). The identical reaction has been proposed by Jada [78] to explain the acid-catalyzed reaction of TEOS and water generated by the reaction of acetic acid with ethanol:

$$H_3C-COOH + C_2H_5OH \overset{H^+}{\rightleftharpoons} H_3C-\overset{O}{\overset{\|}{C}}-O-C_2H_5 + H_2O. \qquad (30)$$

Several factors argue against mechanisms involving siliconium ion intermediates, however. McNeill and coworkers [49] measured the deuterium solvent isotope effect and the activation parameters ΔH^* and ΔS^*. From rate

constants measured in hydrochloric-acid solutions using the stopped flow method, a $k_{H_3O^+}/k_{D_3O^+}$ value of 1.24 was obtained. Rather than a dissociative mechanism, this deuterium isotope effect is in accord with an associative mechanism (as in Eq. 25 or 27) in which the silicate monomer is protonated (deuterated) in a rapid first step followed by attack of water and generation of alcohol in subsequent, slower, rate-limiting steps. From a plot of $\ln(k_{obsd}/T)$ versus $1/T$ (where k_{obsd} is the observed first-order rate constant at temperature T), the entropy of activation was calculated to be $-39\ \text{cal deg}^{-1}\ \text{mol}^{-1}$. This large negative entropy of activation suggests a highly ordered A-2-type transition state with at least one water molecule associated with it [49].

Swain *et al.* [79] compared the hydrolysis behavior of triphenylmethyl fluoride (TMF) and triphenylsilyl fluoride (TSF) under similar conditions. They found that, whereas the hydrolysis of TMF was consistent with a positively charged carbonium ion intermediate, the hydrolysis of TSF was not consistent with a positively charged siliconium ion intermediate but rather an intermediate in which silicon is less positively charged than in the original molecule. They concluded that pentacoordinate intermediates are easy pathways for displacements on silicon that are not available for carbon which cannot expand its valence to include more than eight electrons.

Corriu and Henner [80] have examined the siliconium-ion question and have failed to prove the existence of siliconium ions by physiochemical methods, the preparation of stable salts, or identification of reaction intermediates. They conclude that the high affinity of silicon for nucleophiles explains the failure to prove the presence of such ions, but they point out that it is not possible to completely exclude their existence.

Using ^{29}Si NMR and Raman spectroscopy, Jonas [68], Artaki *et al.* [81], and Zerda and Hoang [71] have investigated the hydrolysis of TMOS (pH ~ 5–7.5) at pressures up to 5 kbar. Their observations that pressure increases the rates of reaction without affecting the distributions of hydrolyzed and/or condensed species are consistent with an associative mechanism involving a pentacoordinate intermediate (transition-state volume, ΔV^*, is negative) rather than a dissociative mechanism in which the rate-determining step is the formation of a tricoordinated siliconium ion plus alcohol (ΔV^* positive).

2.3.5.2. Base-catalyzed Hydrolysis

Under basic conditions it is likely that water dissociates to produce nucleophilic hydroxyl anions in a rapid first step. The hydroxyl anion then attacks the silicon atom. Iler [1] and Keefer [48] propose an S_N2–Si

mechanism in which OH^- displaces OR^- with inversion of the silicon tetrahedron:

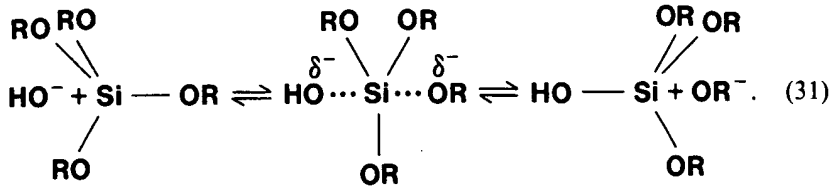

(31)

As discussed for acid-catalyzed hydrolysis, this mechanism is affected by both steric and inductive factors; however steric factors are more important because silicon acquires little charge in the transition state.

Pohl and Osterholtz [50] favor an S_N2^{**}-Si or S_N2^{*}-Si mechanism involving a stable 5-coordinated intermediate.† The intermediate decays through a second transition state in which any of the surrounding ligands can acquire a partial negative charge:

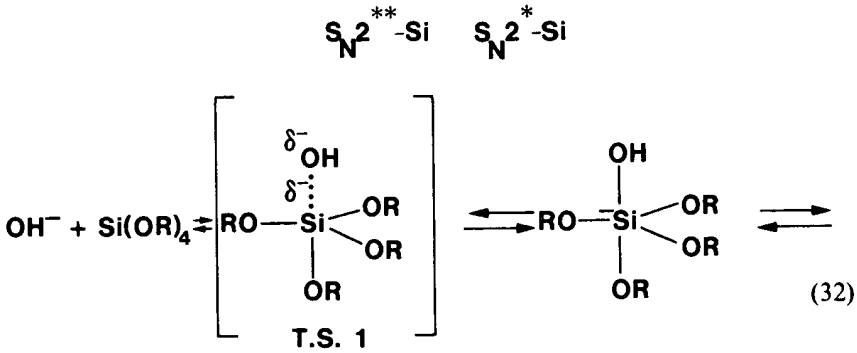

(32)

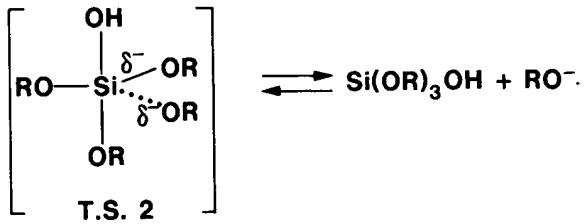

Hydrolysis occurs only by displacement of an alkoxide anion, which may be aided by hydrogen bonding of the alkoxide anion with the solvent (as in Eq. 26).

†The asterisks distinguish between the formation or the decay of the transition states, T.S.1 and T.S.2 as the rate-determining steps, S_N2^{**} and S_N2^{*}, respectively.

Because the silicon acquires a formal negative charge in the transition state, S_N2^{**}-Si or S_N2^{*}-Si mechanisms are quite sensitive to inductive as well as steric effects. Electron-withdrawing substituents such as -OH or -OSi should help stabilize the negative charge on silicon, causing the hydrolysis rate to increase with the extent of OH substitution, whereas electron-providing substituents should cause the hydrolysis rate to decrease (in accord with Fig. 13). Because inversion of configuration is not implicit in Eq. 32, the hydrolysis rate may also increase with the extent of condensation.

The hydrolysis kinetics are expected to be first-order in $[OH^-]$ and second-order with respect to water and silicate (third-order overall kinetics) for all three mechanisms, S_N2-Si, S_N2^{**}-Si, and S_N2^{*}-Si. Therefore, it is generally not possible to distinguish between these mechanisms based on the reaction order.

2.3.6. TRANSESTERIFICATION, REESTERIFICATION, AND HYDROLYSIS

The hydrolysis reaction (Eq. 8) may proceed in the reverse direction, in which an alcohol molecule displaces a hydroxyl group to produce an alkoxide ligand plus water as a by-product. This reverse process, *reesterification*, presumably occurs via mechanisms similar to those of the forward reactions, i.e., by bimolecular nucleophilic substitution reactions: S_N2-Si, S_N2^{**}-Si, or S_N2^{*}-Si. An S_N2^{**}-Si mechanism is shown in Eq. 33 for an acid-catalyzed reesterification reaction:

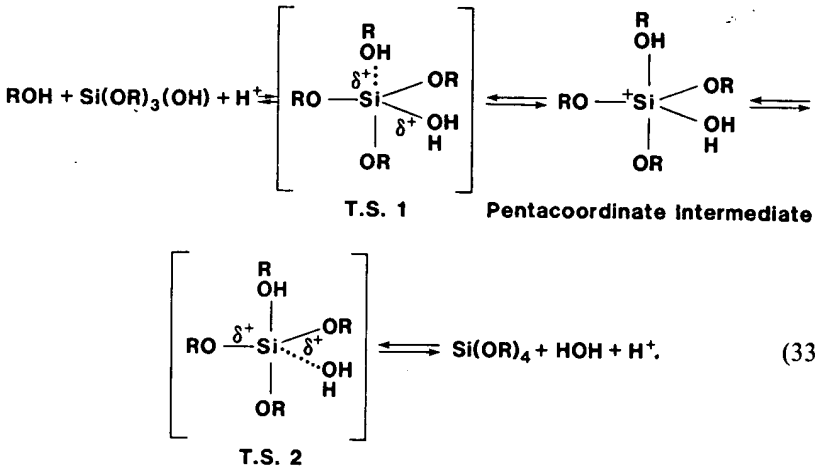

(33)

Voronkov [47], however, proposes the formation of an active six-membered transition complex that contains two alcohol molecules.

Observations of the extent of reesterification of polysiloxanes [e.g., 26,59] indicate that it proceeds much further under acidic conditions than under basic conditions. This led Keefer [48] to the conclusion that the base-catalyzed mechanism involves inversion of configuration, while the acid-catalyzed mechanism does not. It is likely that the first step of the acid-catalyzed reesterification reaction involves the protonation of a silanol group, whereas under base-catalyzed conditions the first step is the deprotonation of an alcohol to form the nucleophile, OR^-. Therefore, the tendency for reesterification to be more complete under acidic than basic conditions may also result from the greater ease of protonation of silanol groups under the acidic conditions normally employed in sol-gel processing (pH ~ 1-3)† than deprotonation of alcohols under the weakly basic conditions normally employed (pH ~ 8-10).

Reesterification is quite important during drying of gels, because in many solvent systems (e.g., ethanol or propanol) excess water can be completely removed via the azeotrope, which has a higher vapor pressure than the neat solvent or water. Keefer [48] has calculated the number of silanols reesterified for several common gel-forming conditions and degrees of condensation. According to these calculations, it is easy to understand the common and contradictory observations that although hydrolysis readily goes to completion with slight excesses of water under acidic conditions, the dried gel may be substantially esterified [26,59].

Transesterification, in which an alcohol displaces an alkoxide group to produce an alcohol molecule:

$$R'OH + Si(OR)_4 \rightarrow Si(OR)_3OR' + ROH \qquad (34)$$

has been extensively studied, because it is the common method of producing various alkoxides of silicon [82]. As discussed by Voronkov *et al.* [47], a wide range of catalysts have been employed, although information on the relative catalytic activity is sparse.

In sol-gel processing, transesterification often occurs when alkoxides are hydrolyzed in alcohols containing different alkyl groups. For example, Brinker *et al.* [59] observed substantial ester exchange during the acid-catalyzed hydrolysis of TEOS in *n*-propanol. Transesterification will also be important in multicomponent systems that employ several alkoxides with differing alkoxide substituents. After transesterification has occurred, subsequent hydrolysis kinetics will depend on the steric and inductive characteristics of the exchanged alkoxide. For example, displacement of ethoxide by *n*-propoxide groups in TEOS was shown to reduce the overall hydrolysis rate [59].

† pH is not well defined in nonaqueous solutions. Often it is a measured value (via a nonaqueous pH electrode) rather than exactly $-\log[H^+]$.

It is suggested that transesterification proceeds by a type of nucleophilic displacement reaction (either S_N2-Si, S_N2^{**}-Si, or S_N2^{*}-Si) similar to reesterification except that an alcohol molecule rather than a water molecule is displaced. As such, transesterification should be subject to both steric and inductive effects. For example, Table 8 indicates that the extent of transesterification is severely reduced when bulky secondary or tertiary alcohols are employed. Investigations by Uhlmann *et al.* [84] and Peace *et al.* [83] show that under acidic conditions, transesterification occurs more readily after partial or complete hydrolysis of the silicate species has occurred, suggesting possible steric constraints. Similar to the case of reesterification, Yamane *et al.* [85] observed transesterification of TMOS under acid-catalyzed conditions but not under base-catalyzed conditions.

From studies of optically active organosilicon compounds, it has been established that transesterification can proceed with retention or inversion of configuration depending on the nature of the leaving group, the solvent, and the catalyst [47]. Because alkoxide substituents are poor leaving groups (alcohols have a $pK_a > 10$), Voronkov *et al.* proposed that only in very polar solvents can there be sufficient separation of charge in the transition state to realize the S_N2-Si mechanism that proceeds with inversion of configuration [47]:

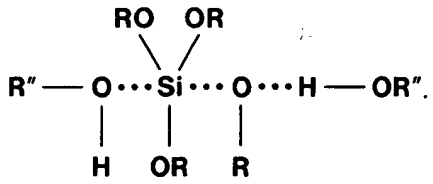

(35)

In less polar solvents, retention of configuration is generally observed. In sol-gel systems, we expect that transesterification of highly condensed species will proceed generally with retention of configuration.

Table 8.

Extent of Hydrolysis and Alcohol Exchange for Acid-Catalyzed Hydrolysis of TEOS in Different Solvents.

Solvent	Hydrolysis (%)	Exchange (%)
Methanol	76	44.7
Cellosolve (ethylene glycol mono ethyl ether)	63	45.9
Isopropanol	63	35.2
t-butanol	67	0

Source: Peace *et al.* [83].

proceeds by a type of nucleophilic
S_N2^{**}-Si, or S_N2^{*}-Si) similar to
lecule rather than a water molecule
should be subject to both steric and
indicates that the extent of trans-
ulky secondary or tertiary alcohols
an *et al.* [84] and Peace *et al.* [83]
sesterification occurs more readily
the silicate species has occurred,
nilar to the case of reesterification,
rification of TMOS under acid-
-catalyzed conditions.
nosilicon compounds, it has been
roceed with retention or inversion
e of the leaving group, the solvent,
ubstituents are poor leaving groups
al. proposed that only in very polar
on of charge in the transition state
oceeds with inversion of configura-

$$\cdots H \text{---} OR''. \qquad (35)$$

uration is generally observed. In sol-
cation of highly condensed species
configuration.

Exchange for Acid-Catalyzed
Different Solvents.

rolysis (%)	Exchange (%)
76	44.7
63	45.9
63	35.2
67	0

Isotopic labelling investigations have confirmed that silanols can be hydrolyzed. When triethylsilanol is hydrolyzed in oxygen-labelled water in the presence of acid or base catalyst or under neutral conditions, the oxygen of the silanol is completely replaced by the water oxygen [47].

$$H_2{}^{18}O + (RO)_3SiOH \rightarrow (RO)_3Si{}^{18}OH + H_2O. \qquad (36)$$

This reaction is generally not important in influencing structural development in sol-gel systems; however it does emphasize that all substituents attached to silicon are quite labile and will depend in an equilibrium sense on the changing concentrations of alcohol and water as well as the solvent, nature of the catalyst, and extent of condensation.

2.4. Condensation

Polymerization to form siloxane bonds occurs by either an alcohol-producing condensation reaction (Eq. 9) or a water-producing condensation reaction (Eq. 10). The latter reaction has been discussed in detail by Iler [1] with regard to forming silicate polymers and gels in aqueous media. Engelhardt and coworkers [21] employed ^{29}Si NMR to investigate the condensation of aqueous silicates at high pH. Their results indicate that a typical sequence of condensation products is monomer, dimer, linear trimer, cyclic trimer, cyclic tetramer, and higher-order rings. As discussed in Section 1, the rings form the basic framework for the generation of discrete colloidal particles commonly observed in aqueous systems [1].

This sequence of condensation requires both depolymerization (ring opening) and the availability of monomers, which are in solution equilibrium with the oligomeric species and/or are generated by depolymerization (reverse of Eqs. 9 and 10). However in alcohol–water solutions normally employed in sol-gel processing, the depolymerization rate is lower than in aqueous media, especially at low pH [1]. Under these conditions, Iler [1] proposed:

> Where depolymerization is least likely to occur so that the condensation is irreversible and siloxane bonds cannot be hydrolyzed once they are formed, the condensation process may resemble classical polycondensation of polyfunctional organic monomer resulting in a three dimensional molecular network. Owing to the insolubility of silica under these conditions the condensation polymer of siloxane chains cannot undergo rearrangement into particles.

This is quite a prophetic statement with regard to the sequence of condensation reactions in sol-gel systems where, depending on conditions, a complete spectrum of structures ranging from molecular networks to colloidal particles may result.

2.4.1. EFFECTS OF CATALYSTS

Although the condensation of silanols can proceed thermally without involving catalysts, their use especially in organosilanes is often helpful. Numerous catalysts have been employed: generally compounds exhibiting acid or base character but also neutral salts and transition metal alkoxides, e.g. $Ti(OEt)_4$ [86]. In sol-gel systems mineral acids, ammonia, alkali metal hydroxides, and fluoride anions are most commonly used. As discussed in the section on hydrolysis, the understanding of catalytic effects is often complicated by the increasing acidity of silanol groups with the extent of hydrolysis and polymerization, and by the effects of reverse reactions that become increasingly important with greater concentrations of water and/or base.

Pohl and Osterholtz [50] used ^{13}C and ^{29}Si NMR to investigate the condensation of alkylsilanetriol to bis-alkyltetrahydroxydisiloxane in buffered aqueous solutions as a function of pD ($-\log[D_3O^+]$). The second-order rate constants for the disappearance of the triol are plotted in Fig. 18a as a pD rate profile. The slopes of the plot above and below the rate minimum at pD 4.5 are +1 and −1, respectively, indicating that the condensation is specific acid- and base-catalyzed. Assink [30] investigated the acid-catalyzed condensation of TMOS over a narrow range of pH. He observed that the condensation rate was proportional to $[H_3O^+]$, which is also consistent with specific acid catalysis.

It is interesting to compare the results in Fig. 18a to the pH-dependence of the gel time (Fig. 18b), which is often used as a measure of the overall condensation kinetics for sol-gel systems (gel time $\propto$ 1/(average condensation rate)). According to Fig. 18b, the overall condensation rate is minimized at about pH 1.5 and maximized at intermediate pH. Stable (nongelling) systems are obtained under more basic conditions. The minimum at ~pH 2 corresponds to the isoelectric point of silica: surface silanol groups are protonated and deprotonated at lower and higher pH values, respectively. Because silanols become more acidic with the extent of condensation of the siloxane network to which they are attached, the shift in the minimum rate from ~pD 4.5 (condensation of monomers, $RSi(OH)_3$) to pH 2 (condensation of polydisperse, higher-order polymers leading to gelation) presumably reflects the increasing acidity of silanols with the degree of condensation. Regardless of the cause, the pH-dependence suggests that for more highly cross-linked systems, protonated and deprotonated silanols are involved in the acid- and base-catalyzed condensation mechanisms at pH < 2 and pH > 2, respectively. Under more basic conditions where the gel times are observed to increase (see, e.g., Fig. 5), condensation reactions proceed but gelation does not occur. In this pH regime, particles are formed that, after

Fig. 18.

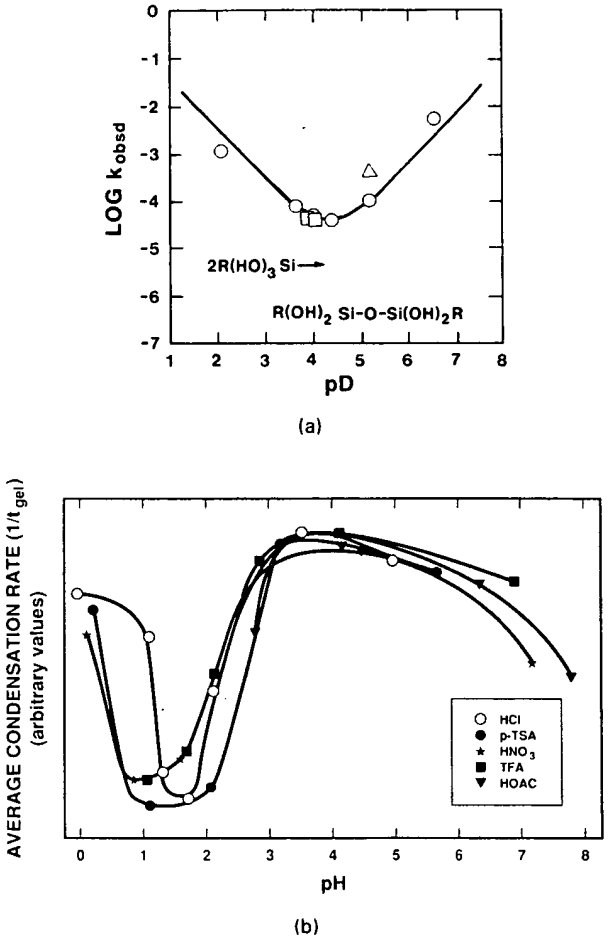

(a) pD-rate profile for the condensation of alkylsilanetriol in buffered aqueous solution [50]. (b) average condensation rates (1/gel times) for TEOS hydrolyzed with solutions of various acids: (*p*-TSA) *p*-toluenesulfonic acid; (HOAc) acetic acid; (TFA) tri-fluoroacetic acid. After Coltrain *et al.* [57].

reaching a critical size, become stable toward gelation due to mutual repulsion effects. This high-pH region represents the conditions in which so-called Stöber silica particles [27] are formed.

In both aqueous and mixed alcohol–water systems, traces of HF have a remarkable catalytic effect on the polymerization rate [87,88]. (See Table 5.) Below pH 2, Iler [1] observed that the polymerization rate is proportional

to the concentration of H^+ and F^-. He proposed that the condensation mechanism may involve a bimolecular intermediate in which the fluorine anion temporarily increases the coordination of one silicon from four to five or six just as in the case of the OH^- ion. Rabinovich and Wood [87] proposed a mechanism in which F^- displaces an OH^-, causing localized attractions to other silanol species, thereby increasing the condensation rate. Because F^- is more electron-withdrawing than OH^-, an alternate argument is that F^- substitution for OH^- reduces the electron density on Si, making it more susceptible to nucleophilic attack, consistent with the view of Corriu *et al.* [56].

2.4.2. STERIC AND INDUCTIVE EFFECTS

During sol-gel processing, condensation can proceed by two different reactions (Eqs. 9 and 10) that can occur between substantially different solution species (monomers, oligomers, etc.), which have undergone different extents of hydrolysis. Therefore, steric and inductive effects are not well documented for tetraalkoxides. According to Voronkov *et al.* [47], the condensation rate of triorganosilanols decreases with increase in the length or branching of the chain of the alkyl radical, or, if aromatic groups are present, with increase in their number. Likewise in tetrafunctional alkoxides normally employed in sol-gel processing, we expect that substituents that increase steric crowding in the transition state will retard condensation. Voronkov *et al.* [47] also say that the condensation rate increases with an increase in the number of silanols on the silicon atom (increasing silanol acidity). This result may be explained on the basis of steric, inductive, or statistical effects.

The previous section indicates that the acid- and base-catalyzed condensation mechanisms involve protonated and deprotonated silanols, respectively. In organosilanes organic substituents influence the acidity of silanols involved in condensation. Electron-providing alkyl groups reduce the acidity of the corresponding silanol. This should shift the isoelectric point toward higher pH values as observed in Fig. 18a, significantly influencing the pH-dependence of the condensation mechanism. Conversely, electron-withdrawing groups (−OH or −OSi) increase the silanol acidity, and the minimum condensation rate for oligomeric species occurs at about pH 2 (as judged from gel times versus pH, Fig. 18b). Thus, the extent of both hydrolysis and condensation and, in organoalkoxysilanes $[R_xSi(OR)_{4-x}]$, the value of x determine the reaction mechanism and define what is meant by acid- or base-catalyzed condensation. In general we refer to base-catalyzed condensation as occurring when the pH is above about 2.

Although inductive effects are clearly important, Voronkov *et al.* state that in acid-catalyzed condensation of dialkysilanediol, steric effects predominate over inductive effects [47]. Therefore, in tetrafunctional alkoxide precursors the inductive effects resulting from longer-chain alkyl substituents are probably even less important.

2.4.3. EFFECTS OF SOLVENT

As discussed in the section on hydrolysis (Section 2.4.3), solvent effects have been primarily evaluated in the context of drying control chemical additives added to facilitate the rapid drying of monolithic gels without cracking. Solvents (or additives) may be either protic or aprotic and may vary in their polarity. (See Table 7.) Depending on the pH, either protonated or deprotonated silanols are involved in the condensation mechanism. Because protic solvents hydrogen bond to nucleophilic deprotonated silanols and aprotic solvents hydrogen bond to electrophilic protonated silanols, protic solvents retard base-catalyzed condensation and promote acid-catalyzed condensation. Aprotic solvents have the reverse effect.

Unfortunately, few data are available to determine unambiguously the effect of solvent type on the condensation rate. Artaki *et al.* [89] investigated the effects of protic and aprotic solvents on the growth rates of polysilicates prepared from TMOS ($r = 10$) with no added catalyst (pH measured immediately after mixing the reactants equalled 6–7). Using Raman spectroscopy and molybdic acid reagent methods (see, e.g., ref. 1), qualitative information related to the size of the polysilicate species was obtained as a function of the reduced time, t/t_{gel}, for five solvent systems: methanol, formamide, dimethylformamide, acetonitrile, and dioxane. Table 9 lists the stabilized

Table 9.

Relative Raman Intensity of 830-cm^{-1} Band, I^{tot}, at $t/t_{gel} = 2$; Inverse Relative Molybdic Acid Rate Constant, K^{-1}, and Gel Times for TMOS Hydrolyzed in Different Solvents.

Solvent	I^{tot}	K^{-1}	t gel (h)
Methanol	1	1	8
Formamide	1.3	1.3	6
Dimethyl-formamide	1.4	1.3	28
Acetonitrile	1.7	1.9	23
Dioxane	2.1	1.9	41

Source: Artaki *et al.* [89].

final intensity, I^{tot}, of the 830-cm^{-1} band (a value proportional to the number of siloxane bonds in the scattering volume†) evaluated at $t/t_{gel} = 2$, the reciprocal molybdenum rate constant, k^{-1} (proportional to the polymer size) evaluated at $t/t_{gel} = 0.8$, and the gel time, t_{gel}, for the five solvent systems.

These solvents may be categorized as polar protic (water, methanol, formamide), polar aprotic (acetonitrile, dimethylformamide) and nonpolar aprotic (dioxane). (See Table 7.) Artaki *et al.* [89] explained that under base-catalyzed condensation conditions (pH > 2.5), the aprotic solvent, dioxane, is unable to hydrogen bond to the SiO^- nucleophile. In addition, because it is nonpolar, it does not tend to stabilize the reactants with respect to the activated complex. Therefore, dioxane should result in a significant enhancement of the condensation rate and cause an efficient condensation leading to the formation of large, compact spherical particles. The polar, aprotic solvents, dimethylformamide and acetonitrile, also do not hydrogen bond to the silicate nucleophile involved in the condensation reaction. However, due to their polarity the anionic reactants are stabilized with respect to the activated complex slowing down the reaction to some extent.

Both methanol and formamide are protic solvents and as such can hydrogen bond to SiO^-, making it less nucleophilic. However, according to Artaki *et al.* [89], formamide is capable of forming significantly stronger hydrogen bonds to the reactant species (dipole moment, μ, equals 3.7 and 1.7 for formamide and methanol, respectively). (See Table 7.) Therefore, compared to methanol, formamide should provide more extensive steric shielding around silicon preventing efficient condensation. This line of reasoning appears inconsistent with the results in Table 9 that show more extensive condensation in the formamide system. This apparent contradiction may be explained by the partial hydrolysis of formamide to produce ammonia plus formic acid [72]. Because base-catalyzed silanol condensation (pH > 2.5) is generally observed to be first-order in $[OH^-]$, ammonia should increase the condensation rate. To elucidate the effects of solvent type on condensation, further work should be performed in buffered solutions as a function of pH.

A second and important effect of the solvent, one that tends to be ignored, is its ability to promote depolymerization, for example, by the reverse of Eqs. 9 and 10. Iler [1] insightfully suggested that under conditions in which depolymerization is suppressed, condensation may lead to molecular

† Note added in proof: Due to a problem with the spectrometer, the 830-cm^{-1} band was probably caused by light scattering rather than Raman scattering. However, since light scattering also is a measure of particle growth, the conclusions of this work are qualitatively correct.

networks, whereas under conditions in which depolymerization is promoted, restructuring occurs ultimately resulting in the formation of highly condensed colloidal particles. Because the nucleophile (OH^-) is involved in the base-catalyzed hydrolysis of siloxane bonds (reverse of Eq. 10), aprotic solvents, which are unable to hydrogen bond to OH^- and therefore make OH^- a stronger nucleophile, promote restructuring leading to more highly condensed species. Enhanced restructuring resulting from the activation of the nucleophile in aprotic systems may further explain the results of Artaki *et al.* [89]. Clearly, further work needs to be performed to elucidate both the effects of solvent reactivity (e.g., the hydrolysis of formamide) and the tendency of the solvent to promote restructuring via enhanced depolymerization. The effects of depolymerization on structural evolution discussed further in Section 2.6.

2.4.4. MECHANISMS

2.4.4.1. Base-catalyzed Condensation

The most widely accepted mechanism for the condensation reac involves the attack of a nucleophilic deprotonated silanol on a ne silicate species as proposed by Iler [1] to explain condensation in aqu silicates systems[†]:

$$SiO^- + Si(OH)_4 \leftrightarrows Si\text{-}O\text{-}Si + OH^-. \quad (37)$$

This reaction pertains above the isoelectric point of silica (>pH 1.5–4.5, depending on the extent of condensation of the silicate species), where surface silanols may be deprotonated depending on their acidity.The acidity of a silanol depends on the other substituents on the silicon atom. When basic OR and OH are replaced with OSi, the reduced electron density on Si increases the acidity of the protons on the remaining silanols [66]. Therefore, Iler's mechanism favors reactions between larger, more highly condensed species, which contain acidic silanols, and smaller, less weakly branched species. The condensation rate is maximized near neutral pH where significant concentrations of both protonated and deprotonated silanols exist. A minimum rate is observed near the isoelectric point. (See Fig. 18b.)

Pohl and Osterholtz [50] and Voronkov *et al.* [47] propose essentially the same mechanism to account for deuteroxide (hydroxyl) anion and

[†] Johnson *et al.* recently proposed a condensation mechanism involving a hydrogen-bonded intermediate that contains a five-coordinate $Si(OH)_5^-$ anionic species. (*J. Am. Chem. Soc.* **111** (1989) 3250).

general base-catalyzed condensation of alkylsilanetriol and alkylsilanediol, respectively.

$$\text{R-Si(OH)}_3 + \text{OH}^- \underset{k_{-1}}{\overset{k_1}{\rightleftharpoons}} \text{R-Si(OH)}_2\text{O}^- + \text{H}_2\text{O} \quad \text{fast}$$

$$\text{R-Si(OH)}_2\text{O}^- + \text{RSi(OH)}_3 \underset{k_{-2}}{\overset{k_2}{\rightleftharpoons}} \text{R-Si(OH)}_2\text{-O-Si(OH)}_2\text{R} + \text{OH}^- \quad \text{slow}$$

$$-d\left[\text{silanetriol}\right]/dt = k_1 k_2/k_{-1} \left[\text{RSi(OH)}_3\right]^2 \left[\text{OH}^-\right] \tag{38}$$

According to Pohl and Osterholtz [50], deuteroxide (hydroxyl) anion reversibly reacts with silanetriol in a rapid first step leading to an equilibrium concentration of *silanolate anion*, $RSi(OH)_2O^-$. Silanolate anion reacts with neutral triol in a slower rate-determining step resulting in dialkyl-tetrahydroxydisiloxane and regeneration of hydroxyl anion. Consistent with this mechanism, the condensation rate is observed to be first-order in deuteroxide anion and second-order in triol, $-d[\text{silanetriol}]/dt = (k_1 k_2/k_{-1})[RSi(OD)_3]^2[OD^-]$. Further condensation of the disiloxane was not observed at short reaction times, presumably due to steric effects.

It is generally believed that the base-catalyzed condensation mechanism involves penta- or hexacoordinated silicon intermediates or transition states [79,81,90–92]. For silicic acid polymerization, Okkerse [90] proposed a bimolecular intermediate involving one hexacoordinated silicon:

$$\text{Si(OH)}_3\text{O}^- + \text{Si(OH)}_4 \rightleftharpoons \text{OH} \text{---} \underset{\text{OH}}{\overset{\text{OH}}{\overset{\text{OH}}{\text{Si}}}} \text{---} \text{O}^- \text{---} \underset{\text{OH}}{\overset{\text{OH}}{\overset{\text{OH}}{\text{Si}}}} \text{---} \text{OH} \tag{39}$$

Grubbs [91] proposed that the condensation of trimethylsilanol in methanol occurs by an S_N2-Si mechanism in which the nucleophile approaches the backside of the silicon which subsequently undergoes displacement of its hydroxyl anion. Swain *et al.* [79] have proposed that silicon

forms stable pentacoordinate intermediates: either S_N2^{**}-Si or S_N2^{*}-Si mechanisms:

S_N2^{**}-Si S_N2^{*}-Si CONDENSATION

$$\equiv SiOH + OH^- \longrightarrow \equiv SiO^- + HOH$$

$$\equiv SiO^- + Si(OR)_4 \longrightarrow$$

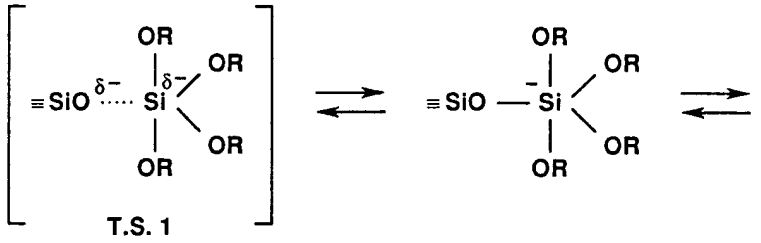

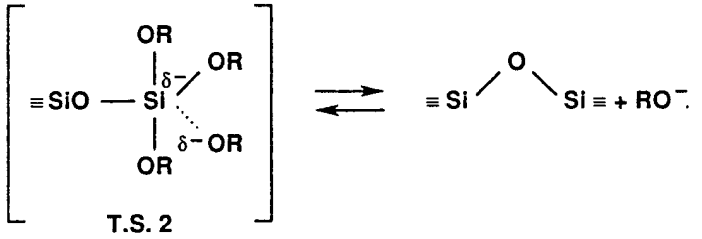

(40)

An associative condensation mechanism involving a penta- or hexacoordinated intermediate is also consistent with the enhanced condensation kinetics observed at high pressures by Artaki *et al.* [81]. (See Fig. 19.) In order to explain these effects, Artaki *et al.* analyzed the activation volumes associated with a base-catalyzed condensation mechanism involving a hexacoordinated intermediate (Eq. 39). They concluded that due to rearrangements of solvent molecules around the anionic nucleophile, SiO^-, and the smaller volume of the transition state compared to the volume of the reactant species, both dissociation of the silanol species and the formation of the transition state contribute to a reduction in the activation volume. Thus, both reactions should be accelerated by pressure. This same reasoning is applicable to mechanisms involving pentacoordinate intermediates.

Using a semi-empirical molecular orbital technique, Davis and Burggraf [92] have examined base-catalyzed silanol polymerization. Their calculations show that water is more easily eliminated when the coordination at silicon can change from hexavalent to pentavalent rather than from pentavalent to tetravalent. These results argue in favor of a condensation mechanism involving a hexacoordinate silicon intermediate. The same reasoning appears

Fig. 19.

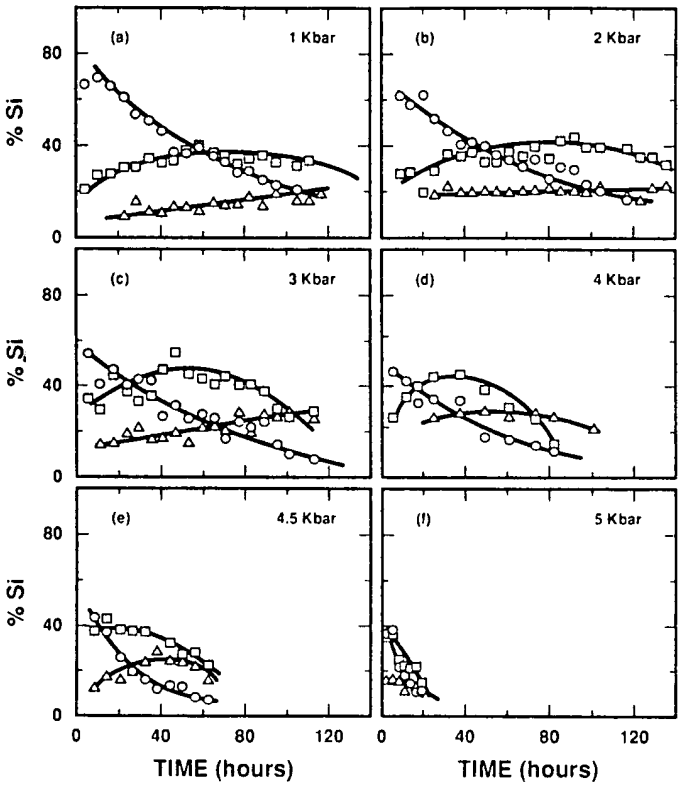

Temporal evolution of all observable condensed species during acid-catalyzed hydrolysis of TMOS. (a) 1 bar, (b) 2 kbar, (c) 3 kbar, (d) 4 kbar, (e) 4.5 kbar, (f) 5 kbar (r = 10); ○: Q^0; □: $(Q^1)_2$, $(Q^1)_3$; △: $Q^1Q^2Q^1$, $(Q^2)_4$ [81].

to apply to base-catalyzed hydrolysis where it may be easier to displace alcohol from a dimer through a hexacoordinated intermediate than from the monomer, implying concerted hydrolysis and dimerization.

2.4.4.2. Acid-catalyzed Condensation

Because in aqueous silicate systems, gel times are observed to decrease below the isoelectric point of silica (Fig. 10b), it is generally believed that the acid-catalyzed condensation mechanism involves a protonated silanol species. Protonation of the silanol makes the silicon more electrophilic and thus more susceptible to nucleophilic attack. The most basic silanol species (silanols

contained in monomers or weakly branched oligomers) are the most likely to be protonated. Therefore, condensation reactions may occur preferentially between neutral species and protonated silanols situated on monomers, end groups of chains, etc. (See also Section 1.2.2 in Chapter 2.)

Pohl and Osterholtz [50] proposed that below about pD 4.5, the increased condensation rate of alkylsilanetriol (Fig. 18a) also involved a deuterated (or protonated) silanol:

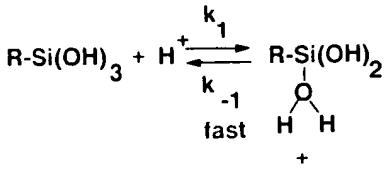

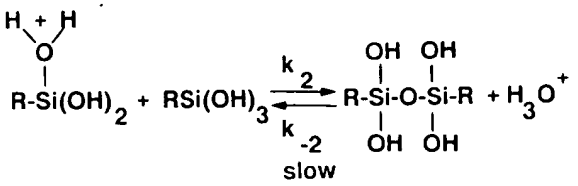

(41)

$$-d[\text{silanetriol}]/dt = k_1 k_2/k_{-1} [RSi(OH)_3]^2 [H^+].$$

Consistent with this mechanism, the condensation rate was observed to be first-order in deuterium ion and second-order in silanetriol. From these results it is not possible to distinguish between S_N2–Si, S_N2^{**}–Si, or S_N2^{*}–Si mechanisms.

Because the proposed reaction mechanisms for both base- and acid-catalyzed condensation involve penta- or hexacoordinate transition states or intermediates, the condensation reaction kinetics will be influenced by both steric and inductive factors. Substituents attached to silicon that reduce steric crowding in the transition state or intermediate will enhance the condensation kinetics. Bulky groups attached to silicon or perhaps partial condensation of the silicon involved in the condensation reaction are expected to retard the condensation process. Replacement of more electron-providing OR groups with progressively more electron-withdrawing OH and OSi groups stabilizes the negative charge on the anionic nucleophile involved in the base-catalyzed condensation reaction and therefore should enhance the kinetics. Similar reasoning leads to the hypothesis that extensive hydrolysis and condensation should destabilize the positively charged intermediate or transition state involved in the acid-catalyzed condensation reaction and thus retard the condensation kinetics.

As discussed for the hydrolysis reaction, the specific mechanism may be influenced by the local environment of the silicon undergoing condensation, the solvent, and nature of the catalyst. For example, Klemperer *et al.* [38] proved that two Q^3 silicon species contained in separate cubic octamers undergo condensation under neutral conditions with essentially complete retention of configuration (see pathway A in Fig. 20), whereas condensation reactions between monomers may result in the inversion of one of the silicate tetrahedra.

2.4.5. EFFECTS OF REVERSE REACTIONS

Alcoholysis and hydrolysis of siloxane bonds (reverse of Eqs. 9 and 10) provide a means for bond breakage and reformation allowing continual restructuring of the growing polymers. The rate of hydrolysis of siloxane bonds (dissolution of silica) exhibits a strong pH-dependence as shown in Fig. 21. Between about pH 3 and 8, the dissolution rate increases by over three orders of magnitude in aqueous solution. Partial replacement of water (pH 9.5) with methanol decreases the solubility by over a factor of 20 as shown in Table 10.

Fig. 20.

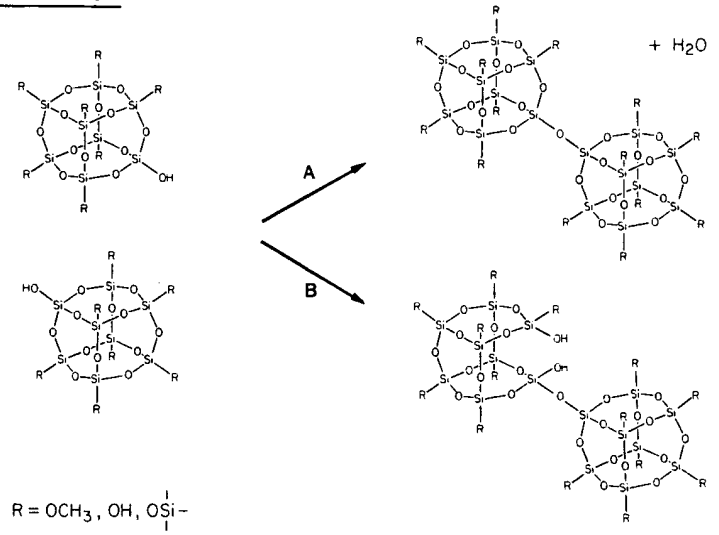

Possible pathways for condensation of Q^3 species contained in cubic octamers. A) With retention of configuration. B) With siloxane bond hydrolysis [38].

Fig. 21.

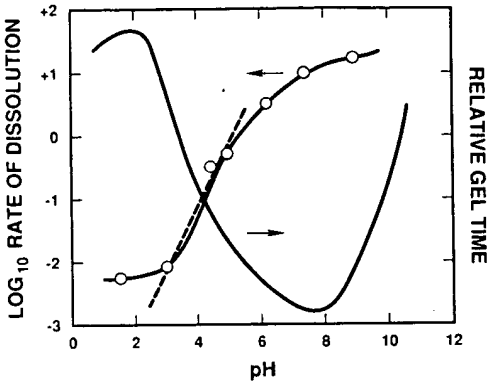

pH-dependence of the dissolution rate and gel times for aqueous silicates [1].

Klemperer and coworkers [93] have shown that alcoholysis occurs under basic conditions, leading to a redistribution of siloxane bonds:

$$\mathrm{ROH + (RO)_3\,Si\text{--}O\text{--}Si(OR)_3 \overset{OH^-}{\rightleftharpoons} Si(OR)_4 + Si(OR)_3\,OH}$$

$$\mathrm{Si(OR)_3\,OH + (RO)_3\,Si\text{--}O\text{--}Si(OR)_3 \rightleftharpoons trimer + ROH}$$

$$\mathrm{2\ dimers \overset{OH^-}{\underset{MeOH}{\rightleftharpoons}} trimer + unhydrolyzed\ monomers.} \qquad \text{REDISTRIBUTION} \qquad (42)$$

Table 10.

Silica Solubility at 25°C in Water-Methanol Solutions.

Wt.% Methanol	Solubility at 25°C (mg l^{-1})
0	140
25	75
50	40
75	15
90	5

Source: Iler [1].

They propose that this reaction accounts for the common observation that under base-catalyzed conditions, unhydrolyzed monomers persist past the gel point even with overstoichiometric additions of water. (See, e.g., ref. 59.) Based on capillary gas chromatography and ^{29}Si NMR results, Klemperer and coworkers [93,94] have shown that the redistribution reactions result in an "inverted" molecular-weight distribution in which high- and low-molecular-weight species are maximized with respect to intermediate-molecular-weight species. As discussed in Section 2.6, this may be explained on the basis of classical nucleation and growth or ripening theories.

According to Iler [1], the dissolution of amorphous silica above pH 2 is catalyzed by OH^- ions that are able to increase the coordination of silicon above four weakening the surrounding siloxane bonds to the network. This general nucleophilic mechanism could presumably occur via S_N2-Si, S_N2**Si, or S_N2*-Si transition states or intermediates and could equally well explain alkoxide ion- or fluorine ion-catalyzed depolymerization mechanisms.

2.5. Sol-Gel Kinetics

Thus far we have discussed the hydrolysis and condensation reactions separately at a rudimentary level that largely ignored how the various functional groups, (OR), (OH), and (OSi), are distributed on the silicon atoms. At this level only three reactions and three rate constants are necessary to describe the functional group kinetics (k_h, $k_{cw}/2$, and $k_{ca}/2$ in equations 43–45), where h is hydrolysis, cw is condensation of water, and ca is condensation of alcohol:

$$\mathrm{SiOR} + \mathrm{H_2O} \xrightarrow{k_h} \mathrm{SiOH} + \mathrm{ROH} \tag{43}$$

$$2\mathrm{SiOH} \xrightarrow{k_{cw}/2} 2(\mathrm{SiO})\mathrm{Si} + \mathrm{H_2O} \tag{44}$$

$$\mathrm{SiOH} + \mathrm{SiOR} \xrightarrow{k_{ca}/2} 2(\mathrm{SiO})\mathrm{Si} + \mathrm{ROH}. \tag{45}$$

In practice, hydrolysis and condensation occur concurrently, and at the nearest functional group level there are 15 distinguishable local chemical environments. Kay and Assink [63,95–97] have represented the 15 silicate species in matrix form as shown in Fig. 22, where the ordered triplet (X, Y, Z) represents the number of -OR, -OH, and -OSi functional groups attached to the central silicon: $Si(OR)_X(OH)_Y(OSi)_Z$, and $X + Y + Z = 4$ = coordination of silicon. At this more sophisticated level, there are 165 distinguishable rate coefficients: $10k_h$, $55k_{cw}$, and $100k_{ca}$, considering only the forward reactions. At the next-to-nearest functional group level, there are 1365 distinct local silicon environments requiring 199,290 rate coefficients [95]!

Fig. 22.

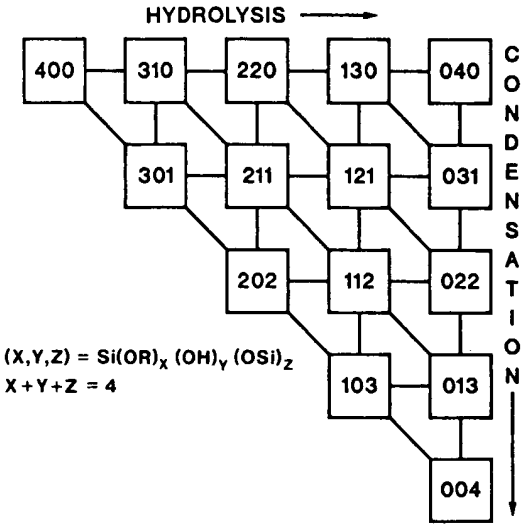

Chemical speciation at next-to-nearest-neighbor level represented in matrix form [63,95,96].

Assink and Kay [63,95–97] have used ^{1}H and ^{29}Si NMR to determine the values of k_h, k_{cw}, and k_{ca} during the initial stages of the acid-catalyzed hydrolysis of TMOS and have considered several kinetic models to explain the temporal evolution of functional groups surounding silicon. The following discussion is largely based on their line of reasoning.

^{1}H NMR is used to measure the relative amounts of methoxy functional groups and methanol molecules as a function of reaction time. Two limiting cases exist. If the hydrolysis rate is much larger than either condensation rate, then the methoxy functional group concentration will quickly be reduced to the value corresponding to complete hydrolysis without condensation. (Reduction in methoxy functional group concentration equals the concentration of added water.) Further reduction in the methoxy functional group concentration occurs at a lower rate commensurate with the overall rate of the condensation reactions. If the hydrolysis rate is much smaller than either condensation rate, hydrolysis will be followed by immediate condensation. In this case, the reduction in methoxy functional group concentration will occur at a rate proportional to the hydrolysis rate. Figure 23 shows the relative methoxy functional-group concentration as a function of time for several values of the initial H_2O/TMOS mole ratio, r. For r values up to 2, the reaction proceeds quickly (in less than three minutes) to the stoichiometry corresponding to complete hydrolysis without condensation.

Fig. 23.

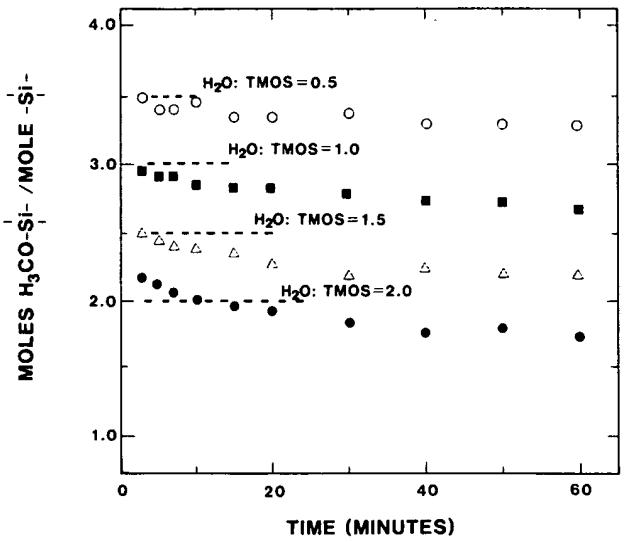

Moles $SiOCH_3$/mole Si versus time for H_2O/Si values ranging from 0.5 to 2.0. Dashed lines are the theoretical values corresponding to complete hydrolysis without condensation [63].

This corresponds to the limiting case in which the initial rate of the hydrolysis reaction is much larger than the sum of the rates of the condensation reactions so that [SiOH] equals the consumption of H_2O by hydrolysis. Based on second-order hydrolysis kinetics (constant $[H_3O^+]$), a lower limit for the hydrolysis-rate coefficient was established as 0.2 l/mole-min) [63].

^{29}Si may be used to determine the rate of formation of Si–O–Si bonds. Again, two limiting cases may be considered based on the equation:

$$d[(SiO)Si]/dt = k_{cw}[SiOH]^2 + k_{ca}[SiOH][SiOR]. \quad (46)$$

If k_{cw} is much greater than k_{ca}, the condensation rate will be proportional to $[SiOH]^2$. If k_{cw} is much smaller than k_{ca}, the condensation rate will be proportional to [SiOH][SiOR]. By measuring the initial overall condensation rate as a function of the initial water concentration, it is possible to determine if either of these limiting cases is applicable.

In the case where the initial overall condensation reaction is negligible with respect to the initial hydrolysis rate and the initial hydrolysis reaction is complete (see Fig. 23), Eq. 46 may be re-expressed as:

$$\frac{d[(SiO)Si]/dt}{\langle[SiOH]\rangle} = (k_{cw} - k_{ca})\langle[SiOH]\rangle + k_{ca}[SiOMe]_o. \quad (47)$$

This expression is valid at early times when the concentration of Si–O–Si is small compared to the initial methoxy functional-group concentration. According to this equation, k_{cw} and k_{ca} are determined from a plot of the initial condensation rate divided by ⟨[SiOH]⟩ versus ⟨[SiOH]⟩ where ⟨[SiOH]⟩ is the average value of the silanol group concentration over the measurement window. (See Fig. 24). k_{cw} and k_{ca} determined from the slope and intercept of this plot are 0.006 and 0.001 l/mole-min, respectively. It is important to note that both the hydrolysis- and condensation-rate coefficients determined for TMOS are significantly greater than corresponding values reported by Pouxviel *et al.* [62] for TEOS. Because increased electron provision by the alkoxide substituents (OEt versus OMe) would be expected to increase the acid-catalyzed hydrolysis- and condensation-rate constants if inductive effects were important, this opposite effect suggests that for tetrafunctional alkoxysilanes, steric rather than inductive factors are more important in determining sol-gel kinetics.

Fig. 24.

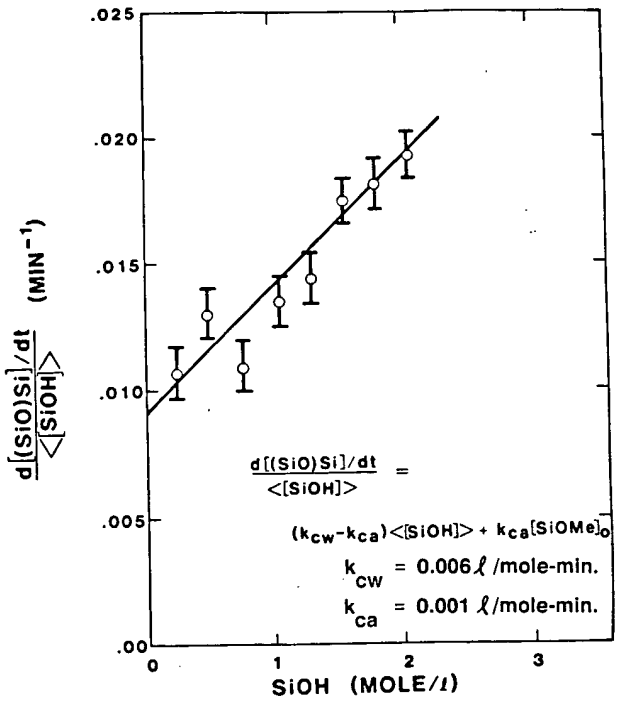

Initial condensation rates divided by the initial silanol concentrations versus the initial silanol concentration. This plot should be linear with a slope of $k_{cw} - k_{ca}$ and intercept of $k_{ca}[\mathrm{SiOR}]_o$ [63].

Fig. 25.

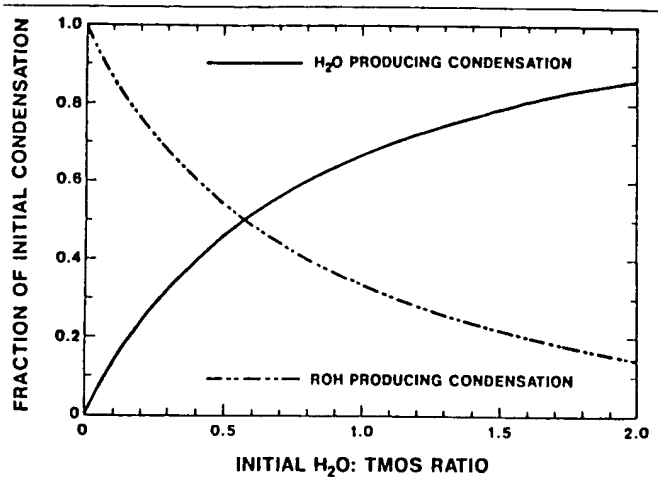

Fraction of condensation occurring by the water-forming reaction or the alcohol-forming reaction versus the initial H_2O : TMOS ratio [63].

Figure 25 shows the fraction of the initial condensation occurring by water- or alcohol-producing reactions as a function of r. The curves are calculated using Eq. 46 and the values of k_{cw} and k_{ca} determined from Fig. 24. It is evident that for small values of r, the alcohol-producing condensation reaction dominates, whereas the water-producing condensation reaction becomes more important when r exceeds about 0.5. Clearly both reactions must be considered to describe condensation kinetics accurately.

To explain the temporal evolution of functional groups surrounding silicon, Kay and Assink [95,63] have considered several kinetic models. When each hydrolysis- and condensation-rate coefficient is much greater than the rate coefficient for the step preceding it, only two of the matrix species will be present, (004) and (400), the relative concentrations of which depend on the H_2O : Si ratio, r. Based on the steric and inductive effects expected for nucleophilic attack of OH^- (hydrolysis) and $\equiv Si\text{-}O^-$ (condensation) on silicon, this situation might occur in base-catalyzed systems [60]. Conversely, when each subsequent rate coefficient is much smaller than the rate coefficient preceding it, the reaction proceeds down the diagonal elements of the matrix [95,63]. Based on the importance of inductive effects, it has been suggested that this situation may occur under acidic conditions, although steric considerations, especially for higher alkoxy groups, may outweigh any inductive effects [60].

A third model assumes that steric and inductive effects are unimportant and that the speciation is governed merely by statistics [95,63]. This model

utilizes two simplifying statistical assumptions: the hydrolysis- and condensation-rate constants depend only on the functional group reactivity, not the local silicon chemical environment; and the rate coefficient for a particular species undergoing one of the three reactions is simply the product of a statistical factor and the appropriate functional group rate coefficient, k_h, k_{cw}, or k_{ca}. For example, the hydrolysis-rate coefficient for species (400) is four times the rate coefficient for species (130), and the water-forming condensation-rate coefficient for species (040) with itself is $4 \times 4 = 16$ times greater than that of species (310) with itself. This reduces the number of rate coefficients required to describe the kinetics at the functional group level from 165 to 3 (k_h, k_{ca}, and k_{cw}).

Kay and Assink used the experimentally determined values of k_h, k_{ca}, and k_{cw} in the statistical model to calculate both the equilibrium distribution of species as a function of r at long reaction times and the temporal evolution of species, during acid-catalyzed hydrolysis of TMOS. The results of these calculations are presented in Figs. 26 and 27 where they are compared to values determined experimentally using ^{29}Si NMR. Agreement between theory and experiment is very good. Because the statistical model implicitly ignores steric and inductive effects as well as reverse reactions such as reesterification, good agreement with experiment suggests that these effects are unimportant for the early stages of hydrolysis and condensation of TMOS at low r values.

Fig. 26.

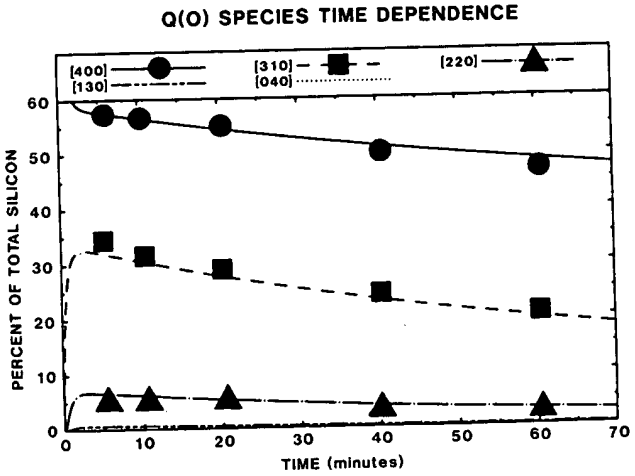

Temporal distribution of Q^0 species during acid-catalyzed hydrolysis of TMOS ($r = 0.5$). Lines are drawn according to the statistical model. Points are experimentally determined by ^{29}Si NMR [96].

Fig. 27.

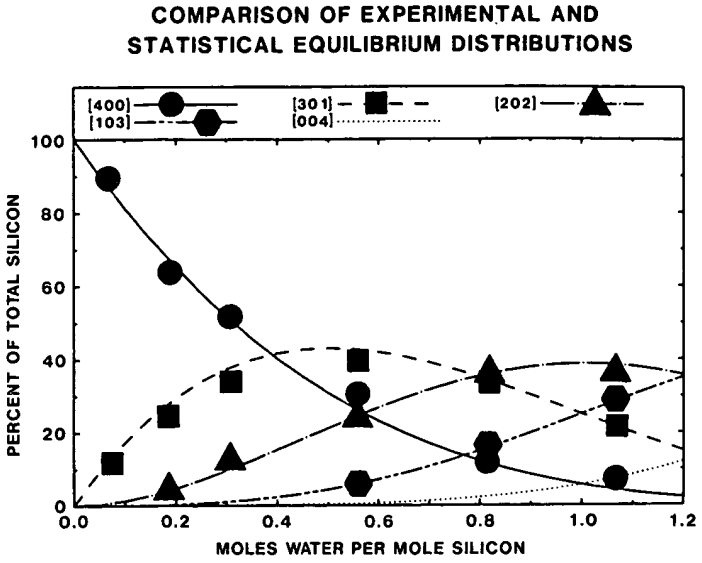

Equilibrium distribution of species at long times: lines drawn according to statistical model; points determined experimentally by ^{29}Si NMR [95].

^{29}Si NMR investigations of the hydrolysis and condensation of TEOS reveal inconsistencies with the statistical model, however. Pouxviel *et al.* [62] report that the relative hydrolysis rate coefficients are 1:5:12:5 compared to 4:3:2:1 (statistical model) for the species (400), (310), (220), and (130), respectively. Lin and Basil [86] do not observe the dimer, (301)–(301), at early times during acid-catalyzed hydrolysis of TEOS, whereas the statistical model predicts its concentration to be ~23% of the total dimer concentration and ^{29}Si NMR shows that it accounts for ~19% of the dimer concentration at early times during the hydrolysis of TMOS [98]. Based on numerical simulations of ^{29}Si NMR data, Pouxviel and Boilot [99] show that the condensation rate decreases with the extent of condensation and that reesterification is significant especially for large values of r.

The rate-constant results [62,86] suggest that as the size of the alkoxide substituents increases or, as the reacting species become more highly condensed, steric effects become increasingly important as observed, for example, in organoalkoxysilanes [47].

Assink (in [100]) has introduced a multiplicative factor ($R < 1$) in the statistical model to account for the reduction in condensation kinetics with the extent of condensation. This modified statistical approach is qualitatively consistent [101] with the rate-constant data of Pouxviel and Boilot.

Although the absence of the (301)-(301) dimer can be rationalized by steric or inductive arguments (the less acidic species, (400) and (310), prefer to condense with the more acidic species, (200), (130), etc., rather than with themselves), the appearance of this species during the latter stages of the reaction, when the water concentration is greatly reduced [86], may indicate that this species hydrolyzes extremely rapidly compared with other species in the TEOS and TMOS systems, or that it forms by reesterification.

Using the kinetic model of Kay and Assink [95], Doughty and coworkers [102] evaluated the temporal evolution of hydrolysis and condensation products of the dimer, hexamethoxydisiloxane, to derive the hydrolysis- and condensation-rate constants defined in Eqs. 43-45. Using ^{29}Si NMR, two types of measurements were performed. The amount of dimer and the extent to which it was hydrolyzed were determined at early times by integration of the Q^1 resonances. The extent of condensation was determined by comparing the integrals of the Q^1 and Q^2 resonances.

The initial rate of formation of siloxane bonds and the average value of the silanol functional-group concentration over the measurement time window determined from the ^{29}Si NMR investigations were used in Eq. 47 to derive the values of the alcohol- and water-producing condensation-rate constants, k_{ca} and k_{cw}, respectively. Calculated values of k_{ca} and k_{cw} are listed in Table 11 where they are compared to the respective values obtained for the monomer, TMOS. The observed rate constants for the alcohol-producing condensation reaction are approximately the same for monomer and dimer (0.001 and 0.0007 l/mol-min, respectively), whereas the rate constants for the water-producing condensation reaction are significantly different (0.006 and 0.0011 l/mol-min, respectively). The differences in the values of k_{cw} obtained for monomer and dimer were explained on the basis of steric and inductive arguments [102]. Bulky OSi groups attached to the silicon undergoing condensation retard the kinetics. Replacement of electron-providing OR groups with more electron-withdrawing OSi groups decreases the stability of the positively charged intermediate also reducing the condensation rate.

Table 11.

Condensation Rate Constants for Methoxy-substituted Monomers and Dimers.

	Q^0 Monomers	Q^1 Dimers
k_{ca} (l/mol-min)	0.001	0.0007
k_{cw} (l/mol-min)	0.006	0.0011

Source: Doughty *et al.* [102].

If the first step in the acid-catalyzed alcohol-producing condensation reaction is the protonation of an alkoxide group, which subsequently becomes the leaving group, MeOH, then the increase in the rate-constant ratio, k_{ca}/k_{cw}, in changing from monomer to dimer condensation (Table 11) suggests that MeOH has become a better leaving group than water as predicted by the partial-charge model [11], or that the electron provision by the R-group predominates over the other (electron-withdrawing) substituents attached to silicon [102].

The statistical model of Kay and Assink appears to be the only available model that predicts the temporal evolution of silicate species during the early stages of the hydrolysis and condensation reactions. For it to be more generally applicable, it must be improved upon to account for steric and inductive effects as well as reverse reactions such as reesterification and siloxane bond hydrolysis.

2.6. Structural Evolution

It is necessary to discuss the structure of silicate solution species on scales of several lengths. On the shortest length scale, the nearest neighbor of silicon may be an alkoxide group (OR), a hydroxyl group (OH), or a bridging oxygen (OSi). On intermediate length scales, oligomeric species (dimers, trimers, tetramers, etc.) may be linear, branched, or cyclic. On length scales large with respect to the monomer and small with respect to the polymer, structures may be dense with well-defined solid–liquid interfaces, uniformly porous, or tenuous networks characterized by a mass or surface fractal dimension, d_f or d_s, respectively [36].

The methods of choice for determining structure on these different-length scales are nonintrusive in situ methods such as nuclear magnetic resonance (NMR) spectroscopy, Raman and infrared spectroscopy, and X-ray, neutron, and light scattering. In the following subsections, structural information obtained by these and other in situ methods are presented in the order of increasing length scales.

2.6.1. NMR INVESTIGATIONS

^{1}H and ^{29}Si nuclear magnetic resonance spectroscopy (NMR) have been employed extensively to elucidate the extent and kinetics of the hydrolysis and condensation reactions accompanying gelation, and the speciation of silicate solutions during the early stages of polymerization of TMOS, TEOS,

Fig. 41b.

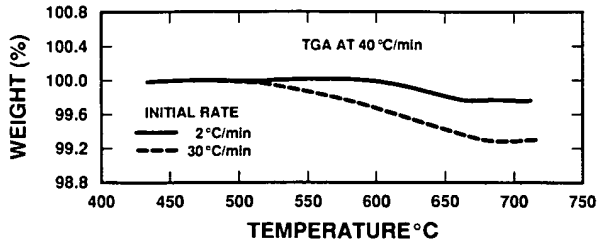

Weight loss measured at 40°C/min for the samples in Fig. 41a previously heated to 525°C at either 2 or 30°C/min [145].

differences in the extent of condensation, depending on the initial heating rate. For there to be equal amounts of shrinkage yet different amounts of condensation, condensation alone cannot account for the region II shrinkage. Therefore it was concluded [145] that at least two shrinkage mechanisms operated concurrently: reduced condensation, resulting from the reduction in time spent at each increment of temperature, was compensated for by increased structural relaxation, causing no heating-rate-dependence of the measured shrinkage.

Because region II shrinkage occurs by concurrent condensation reactions and structural relaxation in the multicomponent gel, the underlying assumption in Eq. 11, that only one shrinkage mechanism predominates, is invalid. A plot of $\ln(\Delta l/l_0)$ versus $\ln(a)$ yields a line of slope 0, requiring n to be infinite. Thus although CHR plots are often composed of essentially linear segments [157] and the changes in slope closely coincide with transitions from region II to region III (suggestive of a change in the predominant shrinkage mechanism), kinetic analyses of CHR data according to Eq. 11 generally do not provide meaningful kinetic parameters describing gel densification. The preceding discussion pertains to region II data. In region III, the concurrence of structural relaxation, continued condensation, and viscous sintering also preclude the use of CHR analyses. This subject is discussed further in Chapter 11.

The DSC curves shown in Fig. 41a provide information concerning the thermodynamics of gel consolidation from which we may infer structural information. These curves result from the exothermic contribution of region III sintering ($-\gamma\,\Delta S$ where γ is the average surface energy and ΔS is the change in surface area) plus the endothermic contributions of (1) the vaporization and subsequent heating of water formed as the by-product of condensation and (2) the heat required to raise the temperature of the skeleton (defined by the heat capacity curves of the fully densified gels). (See Fig. 42.)

Fig. 42.

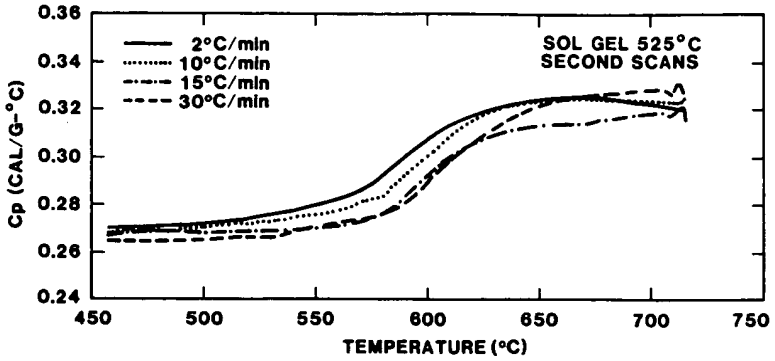

Repeat heat-capacity curves measured at 40°C/min for the samples in Fig. 41a after cooling from 717°C at 80°C/min [145].

It is also necessary to account for the heat of formation of the condensed inorganic product. Estimates of the heats of formation of silicates from silicic acid show the polymerization process to be weakly exothermic as indicated in Eq. 10. However, the change in surface area, heat of vaporation of water, and the heat capacity of the skeleton do not account for the magnitude of the endothermic DSC peaks unless the net contribution of the heat of formation of siloxane bonds, Si–O–Si, is positive [145]. A positive heat of formation associated with condensation is evidence for the formation of strained, cyclic structures as discussed in the following section. Apparently, the progressively larger endotherms that occurred with higher initial heating rates result principally from the larger endothermic contributions of siloxane bond strain (and to a lesser extent, vaporation). Consequently the exotherm expected from sintering is completely obscured at initial heating rates greater than 2°C/min. The endothermic background (400–700°C) observed in Fig. 34b for the two-step acid-catalyzed silicate gel (on which the DSC exotherm associated with structural relaxation is superimposed) is also attributed to the heat of formation of strained, cyclic species.

2.4. Structural Studies of Silicate Gels

The preceding sections have documented that shrinkage in region II results primarily from continued condensation reactions and structural relaxation. The accompanying structural changes have been investigated by vibrational spectroscopy (Raman and IR), solid-state magic angle spinning (MAS) NMR, and electron paramagnetic resonance spectroscopy (EPR).

2.4.1 NMR AND RAMAN SPECTROSCOPIC INVESTIGATIONS OF SILICATE FRAMEWORK STRUCTURES

Brinker and coworkers combined Raman and ^{29}Si MAS NMR spectroscopy with DSC-TGA investigations to elucidate the silicate structures formed by continued condensation reactions in region II [34,160–162]. Figure 43 compares a sequence of Raman spectra of two-step acid–base-catalyzed silica gels (r = 3.8) after drying at 50°C and after heat treatments between 200 and 1100°C. Also shown is the Raman spectrum of conventional vitreous silica (v-SiO_2). Corresponding ^{29}Si MAS NMR and ^{1}H cross-polarization (CP) ^{29}Si MAS NMR spectra are shown in Fig. 44 along with ^{29}Si MAS NMR spectra of the dried or heated gels after exposure to 100% RH water vapor for 24 h at room temperature.

Fig. 43.

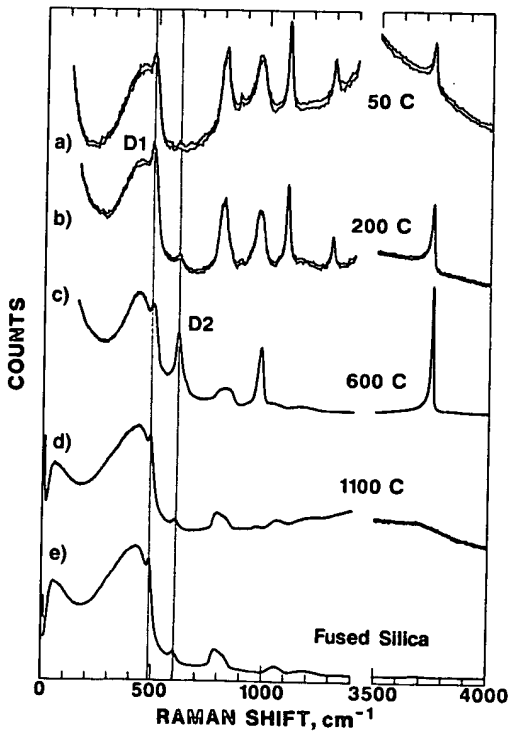

Raman spectra of the two-step acid–base-catalyzed gel (r = 3.8) after drying at 50°C or heating to 200, 600, or 1100°C compared to the spectrum of conventional v-SiO_2. Xerogel samples treated at 50 to 600°C possess high surface areas (>800 m^2/g), whereas the 1100°C sample and v-SiO_2 are fully dense [34].

Fig. 44.

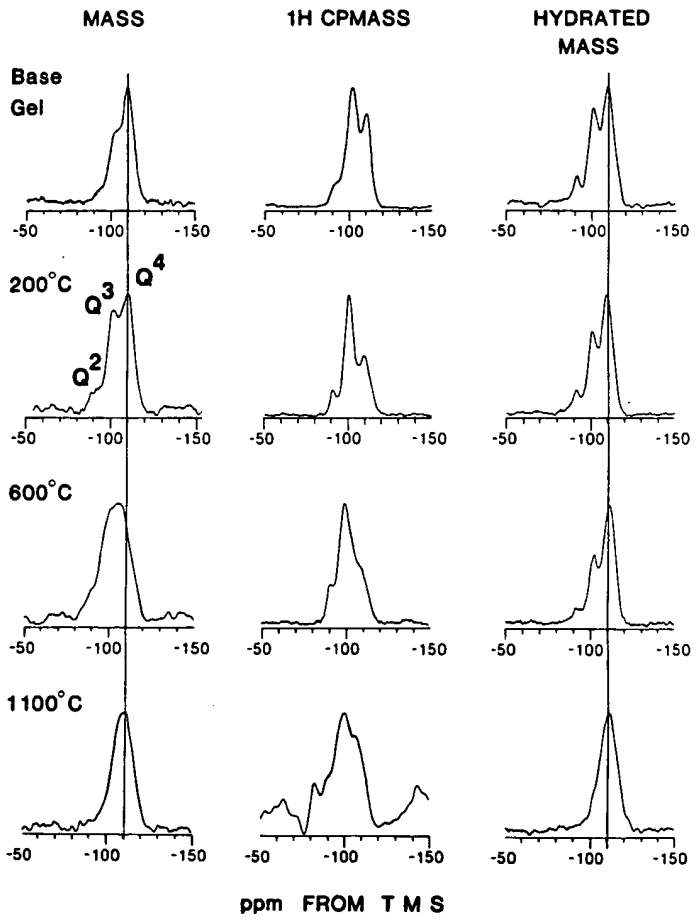

^{29}Si solid-state MAS NMR and ^{1}H cross-polarization MAS NMR spectra of the silica xerogels described in Fig. 43. (Base gel corresponds to the sample dried at 50°C.) The hydrated MAS spectra were collected after exposure of the original samples to 100% RH for 24 hours at 25°C. The ^{1}H CP MAS spectrum of the 1100°C sample is greatly scale-expanded in order to reveal the Q^2 and Q^3 resonances [34].

The SiO_2 framework vibrations that occur at about 430, 800, 1070, and 1180 cm^{-1} in the fused silica spectrum (discussed in Section 1.4.2) can be explained by a vibrational calculation on a *continuous random network* (CRN) [36,37]. The 1070 and 1180 cm^{-1} bands are assigned to the TO and LO modes of the Si-O asymmetric stretching vibration, respectively. Due to the selection rules, Raman-active modes involve symmetric vibrations, which

explains the low relative intensity of these two asymmetric stretching bands. The 800 cm^{-1} band has been assigned to a symmetric Si–O–Si stretching mode. The 430 cm^{-1} band is assigned to a symmetric ring-breathing mode involving mainly oxygen motion. In the following discussion we associate the narrow bands labelled D1 and D2† with small cyclic structures not accounted for in the CRN model: cyclotetrasiloxane (D1) and cyclotrisiloxane (D2). Bands at ca. 3740 and 980 cm^{-1} in the 50, 200, and 600°C samples are assigned to SiO–H and Si–OH stretching vibrations, respectively. The narrow bands at ca. 1100 and 1300 cm^{-1} in the 50 and 200°C samples result from C–H and C–O stretching vibrations of unhydrolyzed ethoxide species often retained under base-catalyzed hydrolysis conditions. (For assignments, see Fig. 20.)

With regard to the framework vibrations, the ca. 430 and 800 cm^{-1} bands are broadened during heating, corresponding to a more varied distribution of Si–O bond lengths and Si–O–Si and O–Si–O bond angles, ϕ and θ, respectively. The band labelled D1 is slightly broadened and exhibits a reduction in relative intensity over the temperature interval 200–1100°C. The band labelled D2 exhibits the most remarkable changes in relative intensity: it is absent after drying at 50°C (Fig. 43a), appears near 200°C (Fig. 43b), becomes quite intense at intermediate temperatures (600–900°C, Fig. 43c), and is reduced in the fully densified gel (1100°C, Fig. 43d) to a level comparable to that in conventional v-SiO_2 (Fig. 43e).

The increase in relative intensity of the D2 band at intermediate temperatures is correlated with a reduction in relative intensity of the ca. 3740 cm^{-1} band assigned to surface SiO–H stretching vibrations [147]. (See Fig. 45.) This suggests that the species responsible for the D2 band forms by condensation reactions involving isolated vicinal silanols on the silica gel surface as confirmed by ^{18}O isotopic enrichment studies [160,161].

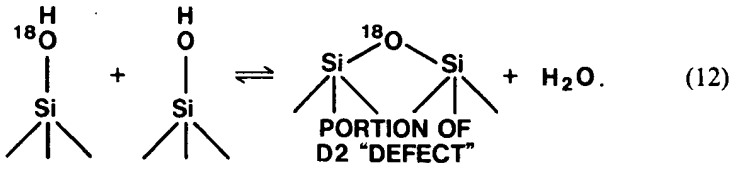

(12)

Further information regarding the structure of the silicate species formed as products of condensation reactions in region II is obtained from the series of ^{29}Si NMR spectra (Fig. 44). The three prominent peaks at chemical shifts of ca. −91, −101, and −110 ppm, corresponding to Q^2, Q^3, and Q^4 sites [163], appear in the MAS and ^1H CPMAS spectra of the gels heated to 50

† The D designation originates from the association of these bands with defects, e.g., broken bonds, in the v-SiO_2 network [65].

Fig. 45.

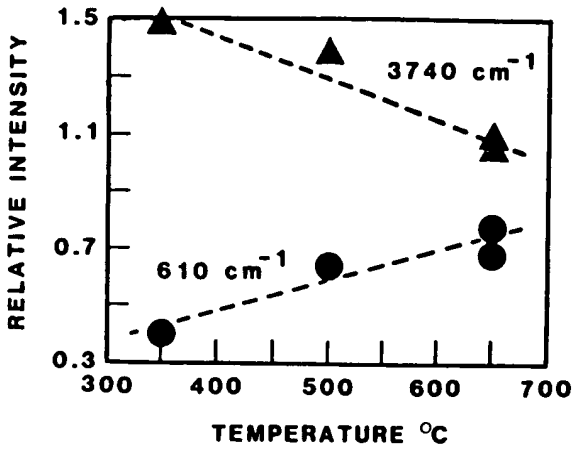

Relative intensities of the 3740 and 610 cm^{-1} Raman bands for the xerogel prepared by two-step acid–base-catalyzed hydrolysis of TEOS (r = 3.8) during heating between 350 and 650°C in air [147].

and 200°C and those rehydrated after heating between 50 and 600°C. Terminal oxygens associated with the Q^2 and Q^3 silicons are bonded to hydrogen (OH groups) as evidenced by the ^1H CPMAS spectra, in which the intensities of the Q^2 and Q^3 sites are enhanced relative to those associated only with bridging oxygens (Q^4 sites) [163,164]. The MAS spectrum of the gel is quite different after heating to 600°C: the Q^3 and Q^4 peaks are not resolved, and there is a broad band of intensity centered at about −107 ppm. A linear relationship exists between the ^{29}Si chemical shift (δ) of Q^4 resonances and the average of the four Si–O–Si angles per Q^4 site (ϕ) [165]:

$$\delta\,(\text{ppm}) = -0.59(\phi) - 23.21. \qquad (13)$$

Accordingly a Q^4 resonance at −107 ppm corresponds to an average ϕ of 142°. Statistically acceptable decomposition of this spectrum, using peak positions of −91 and −101 pm for Q^2 and Q^3 sites requires a peak at about −105 ppm [34]. Because Q^2 and Q^3 sites containing OH groups are not known to resonate in this chemical shift range, the additional peak must be due to a second Q^4 site with a small ϕ value, 138°. The lack of preferential enhancement in this chemical shift range in the ^1H CPMAS spectrum of the 600°C sample indicates that OH is not associated with this site, confirming the assignment to a Q^4 species. Exposure of the 600°C sample to water vapor causes a narrowing and shift of the Q^4 peak position back to its original value in the 50 and 200°C samples.

Heating to 1100°C (region III) completely densifies the gel, reducing its surface area and causing loss of most of the silanol groups as indicated in the Raman spectrum (Fig. 43d). The ^{29}Si MASS NMR spectrum of this sample consists of a Q^4 peak at about -111 ppm corresponding to $\phi = 149°$. ^1H CPMAS yields very little signal for Q^2 and Q^3 sites, consistent with a very low silanol content. The spectrum of the 1100°C sample exposed to 100% RH water vapor is unchanged, indicating the lack of exposed surface area available for rehydration.

The increase in relative intensity of the D2 Raman band correlates well with a reduction in the average Si–O–Si bond angle of Q^4 sites, ϕ, determined from the Q^4 peak positions in the NMR data. D2 is practically absent at 50 and 200°C ($\phi = 148°$), intense at 600°C ($\phi = 138$ and 148°), and quite low in relative intensity after heating to 1100°C ($\phi = 149°$). The relative intensity of D2 is also quite low for the sample exposed to water vapor after heating to 600°C ($\phi = 148°$). By comparison, although the D1 species can form by condensation reactions on the silica gel surface, its formation is not correlated with a reduction in the average value of ϕ.

The association of the species responsible for D2 with the presence of Q^4 sites with reduced values of ϕ and conversely the elimination of this species with an increase in ϕ is consistent with Galeener's [166] assignment of the D2 vibration in conventional v-SiO_2 to an oxygen ring breathing mode of cyclic trisiloxanes (three-membered rings). Galeener made this assignment partly on the basis of the close agreement with the respective oxygen ring breathing frequency of the cyclic molecule, hexamethylcyclotrisiloxane (587 cm^{-1}) [167,168]. Molecular orbital (MO) calculations performed on the model, planar, cyclic molecule, $H_6Si_3O_3$, have established 136.5° and 103° as the optimum values of ϕ and θ, respectively [169]. For all larger rings MO calculations predict optimum angles of $\phi \cong 148°$ (attained by ring puckering) and the tetrahedral angle, $\theta = 109.5°$.

The NMR–Raman data indicate that in gels three-membered rings are absent at low temperatures. They form at intermediate temperatures primarily on the silica gel surface by condensation reactions involving isolated vicinal silanol groups located on unstrained precursors [32]:

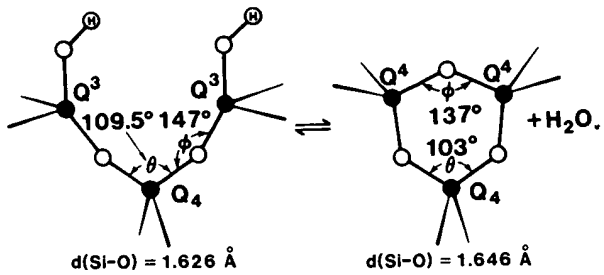

(14)

The cyclic trisiloxanes are composed exclusively of Q^4 silicons as shown by the MAS and ^1H CPMAS spectra of the 600°C sample in which shifts are observed for the Q^4 peak position, whereas the ^1H CPMAS and hydrated MAS spectra show that the Q^2 and Q^3 peak positions are unaffected by the formation or elimination of the D2 species. The H–O distances in the neighboring silanol groups of the precursor (left side Eq. 14) exceeds 5.5 Å, causing them to exhibit SiO–H vibrations characteristic of isolated species [164].

MO calculations [163,165] indicate that a reduction in the value of ϕ below about 140° costs energy, causing the heats of formation of small cyclic molecules to be positive: ΔH_f = 55.4 and 24.4 kcal/(mole of rings) for two-membered (ϕ = 91°) and three-membered rings, respectively. During ring formation according to Eq. 14, all of this energy is associated with ring closure; i.e., the precursor structure is unstrained. Therefore according to theory we expect to measure 24.4 kcal/(mole by-product H_2O) as three-membered rings are formed via dehydroxylation of the silica gel surface. This is close to the value (~23 kcal/mole) found in a careful DSC study [160,161]. This positive heat of formation explains the DSC endotherms (550–650°C) observed in Fig. 41a and the endothermic background (400–700°C) observed in Fig. 34b.

Based on decomposition of the MAS ^{29}Si NMR results (Fig. 44) [170] and estimates of the extent of dehydroxylation according to Eq. 14, the maximum percentage of silicons incorporated in three-membered rings in the two-step acid–base-catalyzed gels studied by Brinker and coworkers exceeds 20%. The NMR results indicate that after heating at intermediate temperatures (e.g., 600°C), the silica gel surface is composed primarily of OH terminated Q^3 sites and two different Q^4 sites with quite different bond angles and bond lengths (Q^4 silicons contained in three-membered rings and Q^4 silicons contained in four-membered and higher-order rings). As discussed in the following chapter, the variations in bond lengths and angles may impart different Lewis acid-base character to the two different Q^4 sites, causing the siloxane bonds contained in the three-membered rings to be very susceptible to hydrolysis. Since the vibrational spectra of dried gels approximates the species distribution present near the gel point, the susceptibility of three-membered rings to hydrolysis also explains the virtual absence of the D2 band in the Raman spectra of xerogels dried at low temperaures. Only in water-starved solutions or very basic conditions (pH > 13 [171]) do cyclic trimers constitute a significant portion of the species population.

The behavior of the D1 vibration in gels appears consistent with its assignment to a four-membered ring: the relative intensity of the D1 band is relatively unchanged by exposure to 100% RH water vapor, and the Q^2–Q^4 peak positions are unaffected by the changing concentrations of the D1

species (Fig. 44),
hydrolysis [167],
in TEOS-derive
oxanes also cont
xerogels. (See, e

Mulder and D
bonded to netw
the D1 band in
tion. This mode
silicate solution
Fig. 38 in Chap
intensity at 490
relative intensit
tion at 600°C [
vibration in co
Therefore it is
vibration at int

Fig. 46.

Raman spe
in oxygen
vacuum (
relatively
treatment

species (Fig. 44). In addition, because cyclic tetrasiloxanes are stable toward hydrolysis [167], they can constitute a large fraction of the oligomeric species in TEOS-derived systems [172]. Thus it is reasonable that cyclic tetrasiloxanes also contribute to the intensity of the D1 band in the low-temperature xerogels. (See, e.g., the 50 and 200°C samples in Fig. 43.)

Mulder and Damen [38] have proposed localized vibrations of O atoms bonded to network terminating Q^3 sites as an alternate structural model for the D1 band in "wet" gels and in high-surface-area gels prior to consolidation. This model is consistent with ^{29}Si NMR and Raman investigations of silicate solutions during the latter stages of polymerization [173]. (See Fig. 38 in Chapter 3.) Although Q^3 silanols most likely contribute to the intensity at 490 cm^{-1} (especially in gels that have not been heated) [34], the relative intensity of the D1 vibration is unaffected by the silanol concentration at 600°C [174] (see Fig. 46) and Q^3 silanols cannot account for the D1 vibration in conventional v-SiO_2 (which may be substantially OH-free). Therefore it is likely that four-membered rings are responsible for the D1 vibration at intermediate and higher temperatures.

Fig. 46.

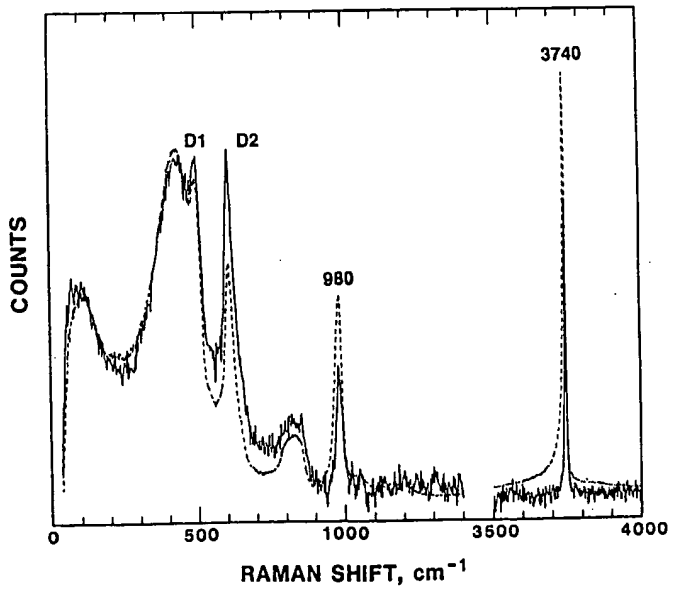

Raman spectra of a two-step acid-base-catalyzed silicate xerogel after heating to 600°C in oxygen for 1 hour (dashed line) or after heating to 600°C in oxygen followed by vacuum (3×10^{-7} torr) for 24 hours (solid line) [174]. The 490 cm^{-1} band (D1) is relatively unchanged although the 980 and 3740 cm^{-1} bands indicate that the vacuum treatment reduces the SiOH concentration by more than 2×

Heat treatments in the vicinity of the glass-transition temperature (T_g) of v-SiO_2 (about 1000°C) reduce the concentrations of the D1 and D2 species to levels comparable to those in conventional v-SiO_2 and cause the $\sim 430\,cm^{-1}$ band to broaden. (See, e.g., the 1100°C spectrum in Fig.43.) From the drastic reduction in the relative intensity of the D2 band (and to a lesser extent the relative intensity of the D1 band), we infer that as the temperature is increased, the reduced viscosity allows the surface to reconstruct by a disproportionation process in which stable five-membered and higher-order rings are formed at the expense of less stable, smaller rings. The assignment of the $\sim 430\,cm^{-1}$ band to O ring-breathing modes of five-membered and higher-order rings is consistent with the broadening observed at 1100° and the trend of decreasing vibrational frequency with increasing ring size (see Table 9) [162].

The effect of viscosity on the surface reconstruction process is evident from Raman investigations of xNa_2O-$(100-x)SiO_2$ gels where $0.1 \leq x \leq 2.0$ [35]. The temperature at which the relative intensity of the D2 vibration (and to a lesser extent the D1 vibration) is suddenly reduced decreases with x in the same manner as T_g. A relationship between viscosity and the relative intensity of the D1 and D2 vibrations was also observed for silica gels by Krol and van Lierop [44]. After heating at 800°C one portion of the sample contained rather large concentrations of the D1 and D2 species characteristic of the surface prior to reconstruction, whereas a second portion of the sample at nominally the same temperature exhibited concentrations of the D1 and D2 species comparable to those in v-SiO_2. Thus within a very narrow temperature or compositional (OH) range the surface suddenly reconstructs forming five-membered and higher-order rings at the expense of three- and four-membered rings. From these observations, we infer that, once formed, small cyclic species are kinetically stabilized by the exceedingly high matrix viscosity at low and intermediate temperatures.

Table 9.

Si–O Stretching Frequencies of Siloxane Rings in Model Compounds and v-SiO_2.

Functional Group	Source Material	Stretching Frequency (cm^{-1})
≥ 5-fold rings	v-SiO_2/SiO_2 gel	430
4-fold rings	Octamethyl cyclotetrasiloxane	480
3-fold rings	Hexamethyl cyclotrisiloxane	587
2-fold rings	Tetramesityl cyclodisiloxane	873
D1	SiO_2 gel	490
D2	SiO_2 gel	608

Source: Brinker *et al.* [162].

2.4.2. INFRARED INVESTIGATIONS OF FRAMEWORK SILICATE STRUCTURES

Infrared (400–4000 cm^{-1}) spectroscopic investigations of silica gel consolidation have been performed by numerous research groups. (See, for example, refs. [35,146,154].) Due to the selection rules, asymmetric vibrations are infrared allowed, therefore the infrared spectra of silica gels complement the Raman spectra discussed in the previous section. One drawback of IR spectroscopy is that bulk silicates are totally absorbing for wave numbers below about 2400 cm^{-1}, so infrared investigations of the fundamental framework vibrations often require dilution in infrared transparent media such as KBr or Nujol.†

The complementary nature of IR and Raman spectra is apparent from the comparison of the IR and Raman spectra obtained during silica gel consolidation in region II. (For example, compare Fig. 19a and Fig. 47 with Figs. 19b or Fig. 43.) The most intense 1080 and 1220 cm^{-1} bands in the IR spectrum are assigned to the TO and LO modes of the asymmetric $Si-O^-$ stretching vibration, respectively [90]. The corresponding Raman bands are very weak. The 800 cm^{-1} band is assigned to symmetric Si–O stretching and the 460 cm^{-1} band to a Si–O–Si bending mode. Si–OH and SiO–H stretching of terminal silanol groups occurs at 960 cm^{-1} and in the envelope of vibrations centered near 3400 cm^{-1}, respectively. There is no evidence in the IR spectra for symmetric ring breathing modes corresponding to the D1 and D2 vibrations in the Raman spectra.

There is comparatively little information obtainable from the IR spectra concerning the evolution of the silicate network in region II. Above about 200°C the major features of the IR spectra change little with temperature. (See Figs. 19a and 47.) Apart from the sharp spectral features associated with C–H and C–O bending vibrations in the 110°C spectrum of the $r = 1$ gel, there are only subtle spectral changes with the value of r (1–20) used in the gel synthesis procedure [90] (Fig. 47). Continued condensation with increasing temperature is evident from the reduction in the relative intensity of the ~970 cm^{-1} band assigned to Si–OH stretching along with a progressive increase in the frequency of the Si–O stretching vibration for the $r = 1$ gel. This latter trend has been observed in many silicate gels and is interpreted to result from a strengthening of the network through cross-linking. As shown in Fig. 48, the increasing $Si-O^-$ stretching frequency is, in general, strongly correlated with increasing density and physical properties such as microhardness and refractive index. The absence of this

† These procedures may introduce additional H_2O. Therefore studies of hydroxyl content or adsorbed water in KBr- or Nujol-prepared samples may be unreliable.

Fig. 47.

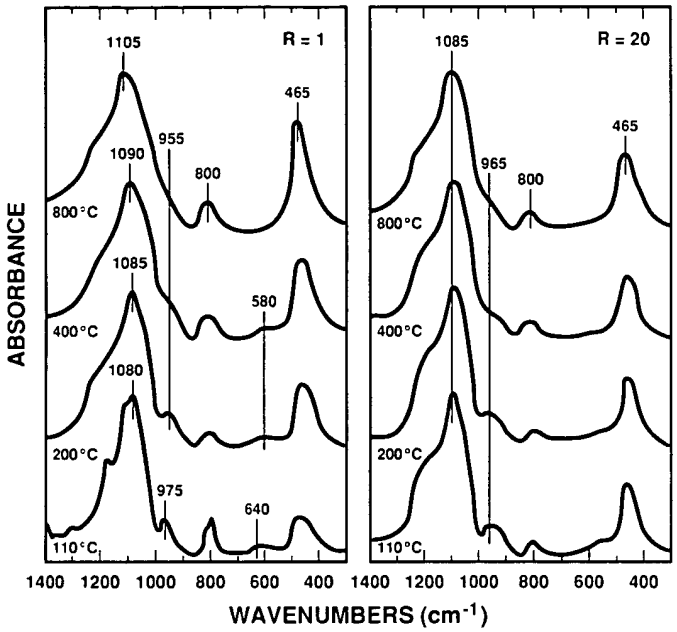

IR spectra of xerogels prepared by single-step hydrolysis of TEOS ($r = 1$ or $r = 20$) after drying at 120°C or after heating between 200 and 800°C [90].

trend at temperatures below 800°C in the $r = 20$ gel (Fig. 47) is evidence that this synthesis condition results in a gel structure composed of extensively crosslinked regions that undergo little further internal condensation in region II. Presumably the stretching frequency of the $r = 20$ gel does increase as the gel densifies by viscous sintering above 800°C in region III.

2.4.3. IR-RAMAN INVESTIGATIONS OF GEL DEHYDROXYLATION

IR (400–4000 cm^{-1}), near-IR (4000–10000 cm^{-1}), and Raman spectroscopy have been used extensively to investigate the dehydroxylation of silica gel surfaces in region II. (See, e.g., refs. [40,41,154].) Figure 49a–c shows infrared spectra of TMOS-derived gels (prepared using a one-step hydrolysis procedure ($r = 4$) under neutral, acidic, or basic conditions) during low-temperature dehydration (25–170°C) [154]. The broad adsorption band between about 3000 and 3800 cm^{-1} corresponds to the fundamental stretching vibrations of different hydroxyl groups. It is composed of a

Fig. 48.

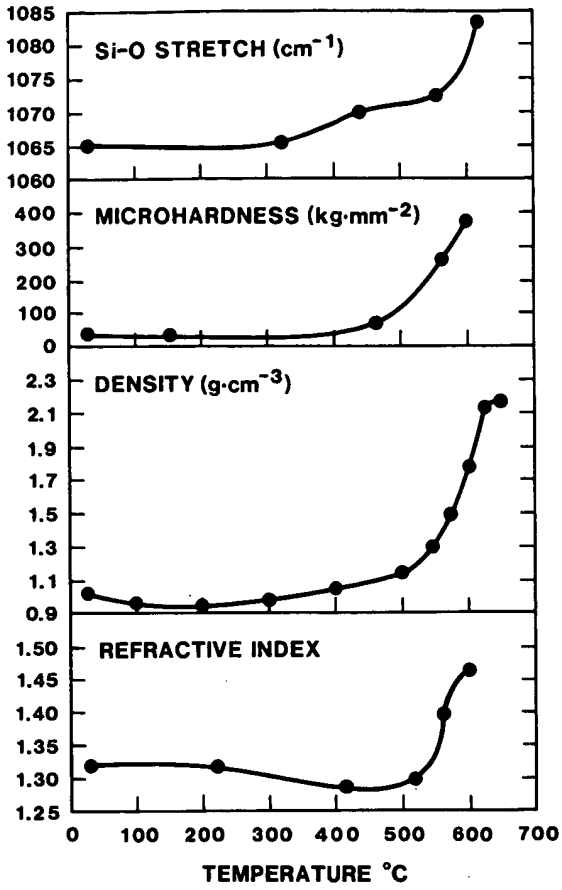

Si-O⁻ asymmetric stretching vibration, microhardness, density, and refractive index of multicomponent borosilicate gels after heat treatments between room temperature and 600°C (heating rates = 0.5–2.0°C/min) [175].

superposition of SiO–H stretching vibrations:

3750 cm^{-1}	isolated vicinal SiO–H stretching
3660 cm^{-1}	mutually H-bonded SiO–H stretching or internal SiO–H stretching
3540 cm^{-1}	SiO–H stretching of surface silanols hydrogen-bonded to molecular water
3500–3400 cm^{-1}	O–H stretching of hydrogen bonded molecular water.

Fig. 49.

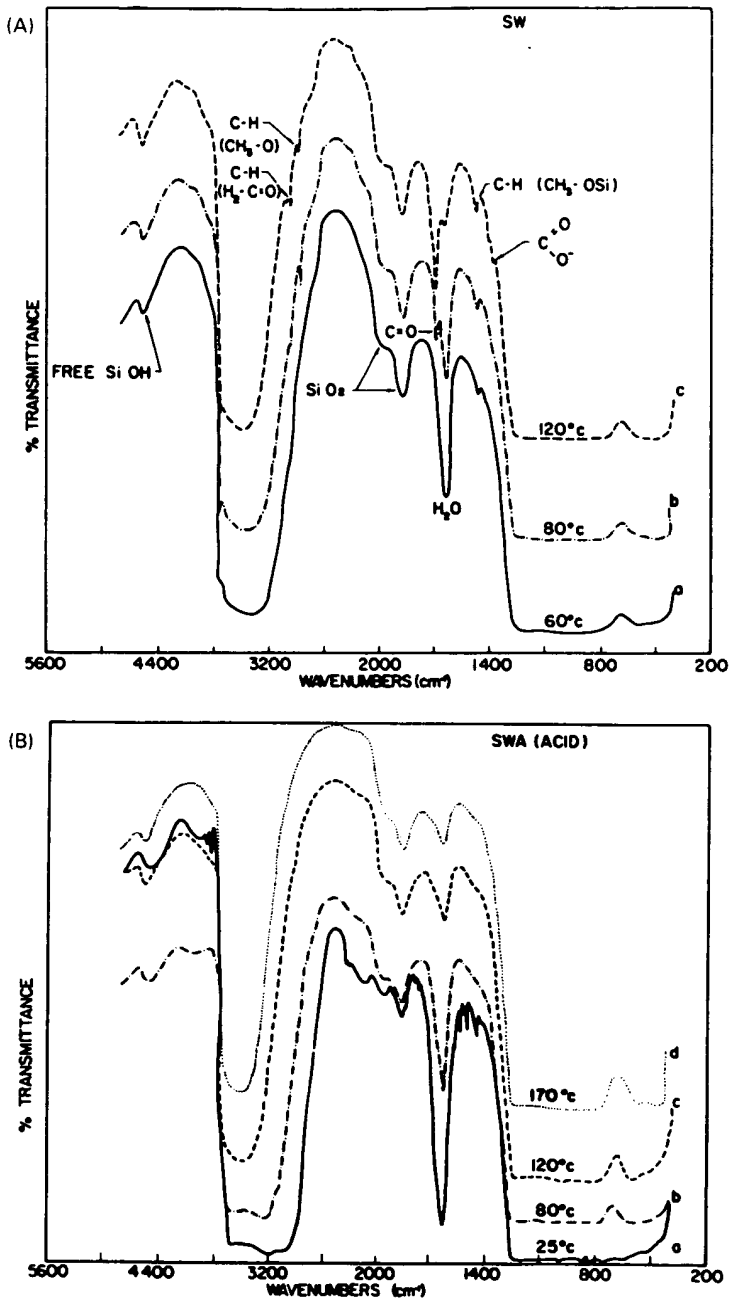
(A)
SW
C-H (CH3-O)
C-H (H2-C-O)
C-H (CH3-OSi)
C=O
FREE Si OH
Si O2
H2O
120°c
80°c
60°c
% TRANSMITTANCE
5600 4400 3200 2000 1400 800 200
WAVENUMBERS (cm-1)
(B)
SWA (ACID)
170°c
120°c
80°c
25°c
% TRANSMITTANCE
5600 4400 3200 2000 1400 800 200
WAVENUMBERS (cm-1)

Fig. 49.

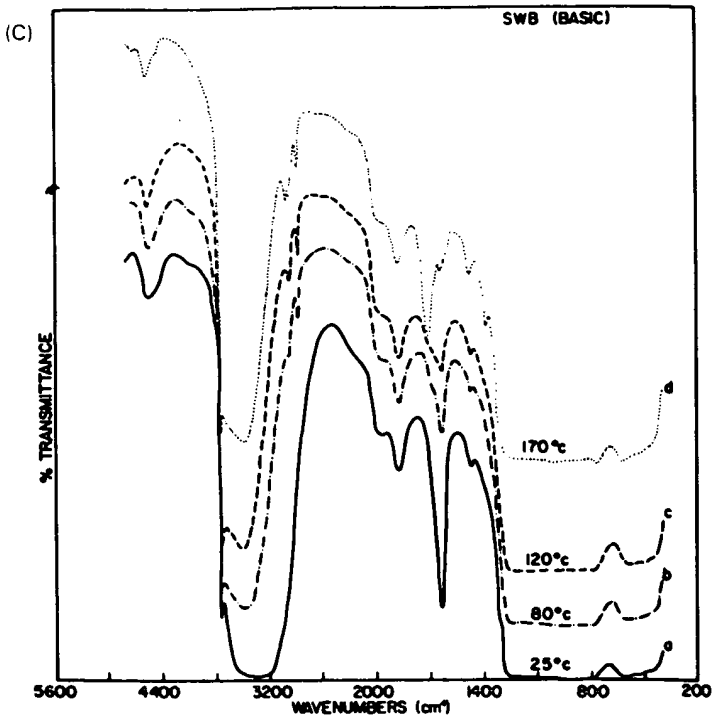

FTIR spectra of xerogels prepared by single-step hydrolysis of TMOS (r = 4) followed by low-temperature heat treatments (60–120°C). (a) SW gel prepared with no added catalyst. (b) SWA gel prepared with 0.1 N HCl. (c) SWB gel prepared with 0.01 N NH_4OH [154].

In addition to the envelope of vibrations corresponding to O–H stretching, the band at 1620 cm^{-1} is assigned to a deformation mode of adsorbed molecular water.

The principal change on heating is a decrease in the concentrations of silanols and adsorbed water. However, the spectra reveal several important differences that depend on the synthesis conditions. The acid-catalyzed gel exhibits the simplest spectrum (Fig. 49b). Above 25°C there is no evidence for C–H stretching vibrations associated with unhydrolyzed methoxy groups (sharp features near 2950 and 1470 cm^{-1} in the neutral and base-catalyzed samples), an indication of complete hydrolysis and no reesterification.†

† This result is quite different from those obtained for one- and two-step acid-catalyzed samples prepared from TEOS [39,40] in which significant reesterification occurred during drying. (See, e.g., Fig. 23.) This may reflect a reduced alcohol–water ratio in the original synthesis procedure.

By comparison, the neutral and base-catalyzed samples (Figs. 49a and 49c) contain unhydrolyzed methoxy groups, because unhydrolyzed monomers and dimers persist long past the gel point under these conditions. (See Chapter 3.) For the neutral and base-catalyzed gels methoxy ligands oxidize to produce formaldehyde and then formic acid and formates that remain strongly bound to the silica surface at temperatures in excess of 300°C. Acid-catalyzed gels contain more internal silanols and, due presumably to their microporous nature, lose water less easily than base-catalyzed or neutral gels. Therefore acid-catalyzed gels generally exhibit lower viscosities than base-catalyzed gels at equivalent temperatures, causing the transition to region III to occur at lower temperatures. (See, e.g., Fig. 27.)

Near-IR spectra are useful in distinguishing between physically adsorbed water and various hydrogen-bonded silanol species. This spectral region is composed of overtones and combination bands associated with various silanol species, adsorbed water, and residual organics. Figure 50 shows a sequence of near-IR spectra obtained during dehydroxylation of an acid-catalyzed TEOS-derived gel [40]. The major spectral features are assigned as follows [40]:

• Triply split bands near 4350 cm^{-1}	combination C–H stretching–deformation
• Triply split bands near 5780 cm^{-1}	first overtone of C–H stretching
• 4566 cm^{-1}	combination stretching–bending of vicinal free SiO H
• 7326 cm^{-1}	first overtone of vicinal free SiOH
• 5290, 5154 cm^{-1}	combination stretching–bending of H-bonded water
• 7142, 6896 cm^{-1}	first harmonic of mutually H-bonded SiO H.

The triply split bands assigned to C–H stretching weaken and disappear near 315°C, the temperature at which the bands assigned to silanols and molecular water exhibit their maximum intensities. The dry gel shows no band at 5290 cm^{-1}, attributable to hydrogen bonded molecular water. This behavior indicates that the dried gel is hydrophobic due to essentially complete esterification of the terminal sites. Heating in air removes the organic groups creating a hydrophilic silanol surface. Further heating causes the intensities of the silanol-related bands to decrease. The reduction in the 7142 cm^{-1} band and the sharpening of the 7326 cm^{-1} band indicate that as

Fig. 50.

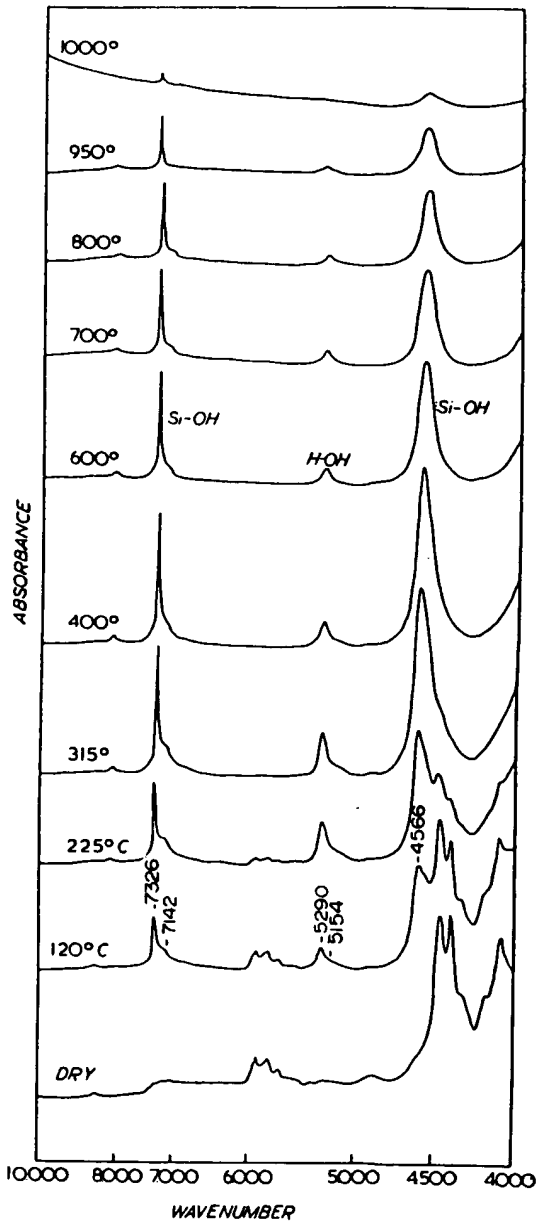

Near IR spectra of xerogels prepared by single-step acid-catalyzed hydrolysis of TEOS and dried at 70°C or heated to temperatures between 120 and 1000°C [40].

temperature is increased, the hydrogen bonded silanols are more easily removed, creating a surface composed primarily of isolated vicinal silanol species.

A sequence of Raman spectra is shown in Fig. 33 for an acid-catalyzed TEOS-derived gel ($r = 10$). The sharp 3750-cm^{-1} band is assigned to SiO–H stretching of isolated vicinal silanols. The broad, low-frequency shoulder (3680 cm^{-1}) is assigned to mutually hydrogen-bonded surface silanols, internal silanols, and/or hydrogen-bonded molecular water. As observed in the near-IR spectra, heating first causes the progressive removal of the low-frequency shoulder, then the removal of isolated silanols. At 800°C some portions of the gel have completely densified causing the formation of a broad band at 3680 cm^{-1} assigned to internal (bulk) silanols. By 900°C the gel is completely densified leaving only internal silanols. By comparison with the v-SiO_2 spectrum (500 ppm OH), the densified gel is estimated to contain 5000 ppm OH.

2.4.4. ELECTRON SPIN RESONANCE STUDIES

Electron spin resonance (ESR) has been used to investigate radiation-induced *paramagnetic defects* in silicate gels after various stages of gel consolidation [176–180]. Paramagnetic defects are not present in unirradiated gels; however their formation during *radiolysis* provides structural information concerning precursor species present in low concentrations (<1%), undetectable by vibrational spectroscopy.

Wolfe *et al.* [178] evaluated the effects of the processing temperature on the types and concentrations of paramagnetic defects in TEOS-derived silica gels. Prior to drying or thermal treatment, the ESR spectra were dominated by a variety of organic radical species (e.g., the ethanol radical, $CH_3CH{\bullet}OH$, and the methyl radical $\bullet CH_3$). Anneals at ~600°C prior to irradiation resulted in substantially lower yields of organic radicals and revealed notable concentrations of *peroxy radicals* (O_2^--type defects). Kordas and coworkers [176,177] observed that vacuum-dried gels prepared from TEOS using a range of r values displayed mainly peroxy radical spectra, regardless of preradiation heat treatments to temperatures up to ~500°C. The seeming ubiquity of the peroxy radical as a radiolysis product has led to the hypothesis that peroxy linkages, Si–O–O–Si, may form as condensation products on the silica gel surface.

Griscom and coworkers [179,180] prepared ^{17}O-enriched and unenriched silica gels from TEOS using a two-step acid–base hydrolysis procedure with $r = 3.8$. After heating, the gels were sealed under vacuum and thereafter not subjected to atmospheric contamination during or after irradiation.